



# Metal-organodiphosphonate chemistry: Hydrothermal syntheses and structures of Zn(II) and Cd(II) coordination polymers with xylyldiphosphonate ligands



Tiffany M. Smith, Diona Symester, Kathryn A. Perrin, Bruce S. Hudson\*, Jon Zubieta\*

Department of Chemistry, Syracuse University, Syracuse, NY 13244, United States

## ARTICLE INFO

### Article history:

Received 16 October 2013

Received in revised form 2 December 2013

Accepted 8 December 2013

Available online 12 December 2013

### Keywords:

Zn(II) and Cd(II) coordination polymers  
Metal-diphosphonate compounds  
Low dimensional metal-diphosphonates through ancillary ligand incorporation  
Crystal structures.

## ABSTRACT

Hydrothermal reactions of zinc(II) acetate dihydrate or cadmium(II) nitrate tetrahydrate with xylyldiphosphonic acid isomers in the presence of an organonitrogen chelating ancillary ligand provided a series of materials of the (M(II)-organonitrogen chelate)/xylyldiphosphonate family. One-dimensional structures were observed for [Zn(H<sub>2</sub>O)(bpy)(1,2-HO<sub>3</sub>PC<sub>8</sub>H<sub>8</sub>PO<sub>3</sub>H)] (1), [Zn(bpy)(1,3-HO<sub>3</sub>PC<sub>8</sub>H<sub>8</sub>PO<sub>3</sub>H)]·H<sub>2</sub>O (2·H<sub>2</sub>O), [M(o-phen)(1,3-HO<sub>3</sub>PC<sub>8</sub>H<sub>8</sub>PO<sub>3</sub>H)] (M = Zn (5·H<sub>2</sub>O), M = Cd (11), and [Zn(tpyprz)(1,2-HO<sub>3</sub>PC<sub>8</sub>H<sub>8</sub>PO<sub>3</sub>H)] (7), while the phases [M(bpy)<sub>2</sub>(1,4-H<sub>2</sub>O<sub>3</sub>PC<sub>8</sub>H<sub>8</sub>PO<sub>3</sub>H<sub>2</sub>)(1,4-HO<sub>3</sub>PC<sub>8</sub>H<sub>8</sub>PO<sub>3</sub>H)] (M = Zn (3) and Cd(9)) exhibited virtual layered structures constructed from {M(bpy)<sub>2</sub>(1,4-H<sub>2</sub>O<sub>3</sub>PC<sub>8</sub>H<sub>8</sub>PO<sub>3</sub>H<sub>2</sub>)<sub>n</sub>}<sup>2n+</sup> chain hydrogen-bonded to the {HO<sub>3</sub>PC<sub>8</sub>H<sub>8</sub>PO<sub>3</sub>H}<sup>2-</sup> charge compensating anions. The two-dimensional structures are represented by [M(o-phen)(1,2-HO<sub>3</sub>PC<sub>8</sub>H<sub>8</sub>PO<sub>3</sub>H)] (M = Zn (4) and Cd (10)) and [Cd(bpy)(1,3-HO<sub>3</sub>PC<sub>8</sub>H<sub>8</sub>PO<sub>3</sub>H)] (8). Expansion into three-dimensions occurs only with the spatially extended 1,4-xylyldiphosphonate ligand in [Zn<sub>4</sub>(o-phen)<sub>4</sub>(1,4-HO<sub>3</sub>PC<sub>8</sub>H<sub>8</sub>PO<sub>3</sub>)<sub>2</sub>(1,4-HO<sub>3</sub>PC<sub>8</sub>H<sub>8</sub>PO<sub>3</sub>H)]·3H<sub>2</sub>O (6·3H<sub>2</sub>O) and [Cd(o-phen)(1,4-HO<sub>3</sub>PC<sub>8</sub>H<sub>8</sub>PO<sub>3</sub>H)] (12).

© 2013 Elsevier B.V. All rights reserved.

## 1. Introduction

Organic–inorganic hybrid materials have enjoyed significant contemporary interest because of the diversity of their structural chemistry [1–3] and their potential applications to catalysis, optics, sorption, separation and magnetism [4–9]. The designed synthesis of such hybrid materials requires appropriate ligands, and carboxylates and polypyridyl ligands have been exploited most commonly in this respect [10–15]. However, while organophosphonate ligands have not been as extensively explored, metal-organophosphonate complexes represent prototypical organic–inorganic hybrid materials. Since the first reports of layered metal-organophosphonates in the early 1970s, Clearfield has pioneered the use of phosphonate ligands in transition metal chemistry [16–18]. These studies and those of other researchers have established an unusual compositional range and rich structural chemistry [19–30] and potential and realized applications to sorption, catalysis, cation exchange, sensors and non-linear optics [31–35]. The magnetic properties of metal-organophosphonate materials have also received considerable attention [36–38].

The family of  $\alpha$ ,  $\omega$ -alkyldiphosphonates has been extensively studied and shown to typically form three-dimensional frameworks, characterized as “pillared layer” materials whose interlamellar separations may be modified by variations of tether lengths. In pursuing our systematic investigations of metal-organophosphonate chemistry [39–59], we have recently turned our attention to the relatively unexplored xylyldiphosphonate ligands [60–67]. In an effort to avoid the common pillared layer structural prototypes such as [M(HO<sub>3</sub>PRPO<sub>3</sub>H)] or [M<sub>2</sub>(O<sub>3</sub>PRPO<sub>3</sub>)] for divalent metal cations, we have exploited the introduction of ancillary ligands such as bipyridine (bpy), o-phenanthroline (o-phen) or tetra-2-pyridylpyrazine (tpyprz). In this study, we present the syntheses and structures of a series of Zn(II) and Cd(II) complexes of 1,2-, 1,3- and 1,4-xylyldiphosphonates with bpy, o-phen or tpyprz ancillary ligands: [Zn(bpy)(H<sub>2</sub>O)(1,2-HO<sub>3</sub>PC<sub>8</sub>H<sub>8</sub>PO<sub>3</sub>H)] (1), [Zn(bpy)(1,3-HO<sub>3</sub>PC<sub>8</sub>H<sub>8</sub>PO<sub>3</sub>H)]·H<sub>2</sub>O (2·H<sub>2</sub>O), [Zn(bpy)<sub>2</sub>(1,4-HO<sub>3</sub>PC<sub>8</sub>H<sub>8</sub>PO<sub>3</sub>H)(1,4-H<sub>2</sub>O<sub>3</sub>PC<sub>8</sub>H<sub>8</sub>PO<sub>3</sub>H<sub>2</sub>)] (3), [Zn(o-phen)(1,2-HO<sub>3</sub>PC<sub>8</sub>H<sub>8</sub>PO<sub>3</sub>H)] (4), [Zn(o-phen)(1,3-HO<sub>3</sub>PC<sub>8</sub>H<sub>8</sub>PO<sub>3</sub>H)]·H<sub>2</sub>O (5·H<sub>2</sub>O), [Zn<sub>4</sub>(o-phen)<sub>4</sub>(1,4-HO<sub>3</sub>PC<sub>8</sub>H<sub>8</sub>PO<sub>3</sub>)<sub>2</sub>(1,4-HO<sub>3</sub>PC<sub>8</sub>H<sub>8</sub>PO<sub>3</sub>H)]·3H<sub>2</sub>O (6·3H<sub>2</sub>O), [Zn(tpyprz)(1,2-HO<sub>3</sub>PC<sub>8</sub>H<sub>8</sub>PO<sub>3</sub>H)] (7), [Cd(bpy)(1,3-HO<sub>3</sub>PC<sub>8</sub>H<sub>8</sub>PO<sub>3</sub>H)] (8), [Cd(bpy)<sub>2</sub>(1,4-HO<sub>3</sub>PC<sub>8</sub>H<sub>8</sub>PO<sub>3</sub>H)(1,4-H<sub>2</sub>O<sub>3</sub>PC<sub>8</sub>H<sub>8</sub>PO<sub>3</sub>H<sub>2</sub>)] (9), [Cd(o-phen)(1,2-HO<sub>3</sub>PC<sub>8</sub>H<sub>8</sub>PO<sub>3</sub>H)] (10), [Cd(o-phen)(1,3-HO<sub>3</sub>PC<sub>8</sub>H<sub>8</sub>PO<sub>3</sub>H)] (11), and [Cd(o-phen)(1,4-HO<sub>3</sub>PC<sub>8</sub>H<sub>8</sub>PO<sub>3</sub>H)] (12).

\* Corresponding authors. Tel.: +1 315 443 2547; fax: +1 315 443 4070 (J. Zubieta). Tel.: +1 315 443 5805; fax: +1 315 443 4070 (B.S. Hudson).

E-mail addresses: [bshudson@syr.edu](mailto:bshudson@syr.edu) (B.S. Hudson), [jazubiet@syr.edu](mailto:jazubiet@syr.edu) (J. Zubieta).

## 2. Experimental

### 2.1. General procedures

All chemicals were used as obtained without further purification with the exception of *p*-xylene diphosphonic acid, ortho-xylene diphosphonic acid and meta-xylene diphosphonic acid which were synthesized in a similar fashion to the literature method [62] using the respective dibromide starting materials. Zinc(II) acetate dihydrate (98%), cadmium(II) nitrate tetrahydrate (98%), 2,2'-bipyridine (99%), 1,10-phenanthroline (99%), and tetra-2-pyridinylpyrazine (97%) were purchased from Sigma–Aldrich. All syntheses were carried out in 23-mL poly(tetrafluoroethylene)-lined stainless steel containers under autogeneous pressure. The pH values of the solutions were measured prior to and after heating using pHYdrion vivid 1-11<sup>®</sup> pH paper. Water was distilled above 3.0 MΩ in-house using a Barnstead Model 525 Biopure Distilled Water Center.

### 2.2. Synthesis of [Zn(H<sub>2</sub>O)(bpy)(1,2-HO<sub>3</sub>PC<sub>8</sub>H<sub>8</sub>PO<sub>3</sub>H)] (1)

A solution of zinc(II) acetate dihydrate (0.092 g, 0.42 mmol), 2,2'-bipyridine (0.078 g, 0.50 mmol), *o*-xylene-diphosphonic acid (0.080 g, 0.30 mmol), and H<sub>2</sub>O (10 mL, 556 mmol) in the mole ratio 1:1.2:0.7:1324 was stirred briefly before heating to 120 °C for 72 h. The initial and final pH values were 4 and 4, respectively. Colorless blocks suitable for X-ray diffraction were isolated 90% yield. IR (KBr pellet, cm<sup>-1</sup>): 3422(m), 3105(w), 3073(w), 2913(w), 2775(w), 2344(m), 1654(w), 1610(m), 1598(m), 1577(w), 1493(m), 1477(m), 1446(m), 1406(w), 1255(m), 1235(m), 1162(m), 1140(s), 1109(s), 1090(s), 1060(m), 1012(m), 956(m), 938(s), 875(w), 788(m), 768(s), 734(m), 657(w), 597(m), 517(s), 480(s). *Anal. Calc.* for C<sub>18</sub>H<sub>20</sub>N<sub>2</sub>O<sub>7</sub>P<sub>2</sub>Zn: C, 42.9; H, 3.97; N, 5.56. Found: C, 42.6; H, 3.88; N, 5.69%.

### 2.3. Synthesis of [Zn(bpy)(1,3-HO<sub>3</sub>PC<sub>8</sub>H<sub>8</sub>PO<sub>3</sub>H)]·H<sub>2</sub>O (2·H<sub>2</sub>O)

A solution of zinc(II) acetate dihydrate (0.10 g, 0.46 mmol), 2,2'-bipyridine (0.040 g, 0.26 mmol), *m*-xylene-diphosphonic acid (0.080 g, 0.30 mmol), and H<sub>2</sub>O (10 mL, 556 mmol) in the mole ratio 1:0.57:0.65:1209 was stirred briefly before heating to 120 °C for 48 h. The initial and final pH values were 2 and 2, respectively. Colorless blocks suitable for X-ray diffraction were isolated in 40% yield. IR (KBr pellet, cm<sup>-1</sup>): 3537(m), 3454(s), 3059(w), 3029(w), 2924(w), 2344(w), 1637(w), 1606(m), 1597(m), 1442(s), 1272(m), 1199(m), 1175(m), 1125(s), 1046(s), 1022(w), 935(s), 765(s), 736(m), 699(m), 528(s), 482(m). *Anal. Calc.* for C<sub>18</sub>H<sub>20</sub>N<sub>2</sub>O<sub>7</sub>P<sub>2</sub>Zn: C, 42.9; H, 3.97; N, 5.56. Found: C, 43.1; H, 3.67; N, 5.44%.

### 2.4. Synthesis of [Zn(bpy)<sub>2</sub>(1,4-H<sub>2</sub>O<sub>3</sub>PC<sub>8</sub>H<sub>8</sub>PO<sub>3</sub>H<sub>2</sub>)(1,4-HO<sub>3</sub>PC<sub>8</sub>H<sub>8</sub>PO<sub>3</sub>H)] (3)

A solution of zinc(II) acetate dihydrate (0.092 g, 0.42 mmol), 2,2'-bipyridine (0.039 g, 0.250 mmol), *p*-xylene-diphosphonic acid (0.080 g, 0.30 mmol), and H<sub>2</sub>O (10 mL, 556 mmol) in the mole ratio 1:0.6:0.716:1324 was stirred briefly before heating to 120 °C for 72 h. The initial and final pH values were 3 and 3, respectively. Colorless blocks suitable for X-ray diffraction were isolated in 90% yield. IR (KBr pellet, cm<sup>-1</sup>): 3490(s), 3408(s), 3056(w), 2917(w), 2344(w), 1580(s), 1520(m), 1440(s), 1421(w), 1311(w), 1259(m), 1187(m), 1142(m), 1080(s), 990(s), 856(m), 771(m), 566(s), 509(s). *Anal. Calc.* for C<sub>36</sub>H<sub>38</sub>N<sub>4</sub>O<sub>12</sub>P<sub>4</sub>Zn: C, 47.6; H, 4.19; N, 6.17. Found: C, 47.2; H, 4.27; N, 5.99%.

### 2.5. Synthesis of [Zn(*o*-phen)(1,2-HO<sub>3</sub>PC<sub>8</sub>H<sub>8</sub>PO<sub>3</sub>H)] (4)

A solution of zinc(II) acetate dihydrate (0.092 g, 0.42 mmol), 1,10 phenanthroline (0.039 g, 0.216 mmol), *o*-xylene-diphosphonic acid (0.080 g, 0.30 mmol), and H<sub>2</sub>O (10 mL, 556 mmol) in the mole ratio 1:0.51:0.71:1324 was stirred briefly before heating to 120 °C for 48 h. The initial and final pH values were 1 and 1, respectively. Colorless blocks suitable for X-ray diffraction were isolated in 60% yield. IR (KBr pellet, cm<sup>-1</sup>): 3434(m), 1422(m), 1237(w), 1214(m), 1165(w), 1135(s), 1047(w), 1041(s), 937(m), 889(m), 851(m), 791(m), 727(m), 543(m). *Anal. Calc.* for C<sub>20</sub>H<sub>18</sub>N<sub>2</sub>O<sub>6</sub>P<sub>2</sub>Zn: C, 47.1; H, 3.53; N, 5.49. Found: C, 47.1; H, 3.62; N, 5.22%.

### 2.6. Synthesis of [Zn(*o*-phen)(1,3-HO<sub>3</sub>PC<sub>8</sub>H<sub>8</sub>PO<sub>3</sub>H)]·H<sub>2</sub>O (5·H<sub>2</sub>O)

A solution of zinc(II) acetate dihydrate (0.10 g, 0.46 mmol), 1,10 phenanthroline (0.040 g, 0.22 mmol), *m*-xylene-diphosphonic acid (0.080 g, 0.30 mmol), and H<sub>2</sub>O (5 mL, 278 mmol) in the mole ratio 1:0.48:0.65:604 was stirred briefly before heating to 120 °C for 48 h. The initial and final pH values were 3 and 3, respectively. Colorless blocks suitable for X-ray diffraction were isolated in 30% yield. IR (KBr pellet, cm<sup>-1</sup>): 3503(m), 3058(w), 2911(w), 2368(w), 2344(w), 1637(w), 1623(w), 1607(w), 1586(w), 1517(m), 1489(m), 1427(m), 1267(m), 1186(m), 1135(s), 1095(m), 1051(s), 931(s), 866(w), 851(m), 807(m), 728(m), 706(m), 58(w), 594(w), 522(s), 481(m). *Anal. Calc.* for C<sub>20</sub>H<sub>20</sub>N<sub>2</sub>O<sub>7</sub>P<sub>2</sub>Zn: C, 45.5; H, 3.79; N, 5.31. Found: C, 45.6; H, 3.57; N, 5.71%.

### 2.7. Synthesis of [Zn<sub>4</sub>(*o*-phen)<sub>4</sub>(1,4-HO<sub>3</sub>PC<sub>8</sub>H<sub>8</sub>PO<sub>3</sub>)<sub>2</sub>(1,4-HO<sub>3</sub>PC<sub>8</sub>H<sub>8</sub>PO<sub>3</sub>H)]·3H<sub>2</sub>O (6·3H<sub>2</sub>O)

A solution of zinc(II) acetate dihydrate (0.092 g, 0.42 mmol), 1,10 phenanthroline (0.040 g, 0.222 mmol), *p*-xylene-diphosphonic acid (0.080 g, 0.30 mmol), and H<sub>2</sub>O (10 mL, 556 mmol) in the mole ratio 1:0.53:0.714:1324 was stirred briefly before heating to 120 °C for 72 h. The initial and final pH values were 5 and 4, respectively. Colorless blocks suitable for X-ray diffraction were isolated in 90% yield. IR (KBr pellet, cm<sup>-1</sup>): 3482(m), 3054(m), 2908(m), 2344(w), 1660(w), 1623(m), 1579(m), 1513(s), 1425(s), 1250(s), 1200(s), 1162(s), 1078(s), 933(s), 857(s), 726(s), 596(w), 563(s), 518(m), 467(w). *Anal. Calc.* for C<sub>72</sub>H<sub>68</sub>N<sub>8</sub>O<sub>21</sub>P<sub>6</sub>Zn<sub>4</sub>: C, 47.2; H, 3.72; N, 6.12. Found: C, 46.6; H, 3.55; N, 6.11%.

### 2.8. Synthesis of [Zn(tpyprz)(1,2-HO<sub>3</sub>PC<sub>8</sub>H<sub>8</sub>PO<sub>3</sub>H)] (7)

A solution of zinc(II) acetate dihydrate (0.092 g, 0.42 mmol), tetra-2-pyridinylpyrazine (0.085 g, 0.219 mmol), *o*-xylene-diphosphonic acid (0.080 g, 0.30 mmol), and H<sub>2</sub>O (10 mL, 556 mmol) in the mole ratio 1:0.52:0.71:1324 was stirred briefly before heating to 120 °C for 72 h. The initial and final pH values were 4 and 2, respectively. Colorless blocks suitable for X-ray diffraction were isolated in 80% yield. IR (KBr pellet, cm<sup>-1</sup>): 3061(w), 3020(w), 2970(w), 2921(w), 2737(w), 2362(w), 2344(w), 1587(m), 1517(w), 1541(w), 1446(m), 1401(m), 1237(m), 1150(s), 1072(s), 1061(s), 1007(m), 926(s), 797(m), 773(s), 744(m), 634(w), 551(m), 529(s), 494(s). *Anal. Calc.* for C<sub>32</sub>H<sub>26</sub>N<sub>6</sub>O<sub>6</sub>P<sub>2</sub>Zn: C, 53.5; H, 3.62; N, 11.7. Found: C, 53.6; H, 3.66; N, 11.5%.

### 2.9. Synthesis of [Cd(bpy)(1,3-HO<sub>3</sub>PC<sub>8</sub>H<sub>8</sub>PO<sub>3</sub>H)] (8)

A solution of cadmium(II) nitrate tetrahydrate (0.098 g, 0.317 mmol), 2,2'-bipyridine (0.071 g, 0.46 mmol), *o*-xylene-diphosphonic acid (0.080 g, 0.30 mmol), and H<sub>2</sub>O (10 mL, 556 mmol) in the mole ratio 1:0.69:0.95:1753 was stirred briefly before heating to 120 °C for 72 h. The initial and final pH values were 1 and 1, respectively. Colorless rods suitable for X-ray

diffraction were isolated in 90% yield. IR (KBr pellet,  $\text{cm}^{-1}$ ): 3422(m), 3059(m), 2945(m), 2364(w), 2343(w), 1595(m), 1576(w), 1487(m), 1439(s), 1411(w), 1321(s), 1247(m), 1205(m), 1174(s), 1078(w), 1052(s), 1034(s), 915(s), 896(m), 805(m), 762(m), 736(m), 700(m), 649(m), 522(s), 478(m). *Anal. Calc.* for  $\text{C}_{18}\text{H}_{12}\text{N}_2\text{O}_6\text{P}_2\text{Cd}$ : C, 40.5; H, 3.38; N, 5.26. Found: C, 40.3; H, 3.41; N, 5.42%.

#### 2.10. Synthesis of $[\text{Cd}(\text{bpy})_2(1,4\text{-H}_2\text{O}_3\text{PC}_8\text{H}_8\text{PO}_3\text{H}_2)(1,4\text{-HO}_3\text{PC}_8\text{H}_8\text{PO}_3\text{H})]$ (**9**)

A solution of cadmium(II) nitrate tetrahydrate (0.098 g, 0.317 mmol), 2,2'-bipyridine (0.070 g, 0.45 mmol), p-xylene-diphosphonic acid (0.080 g, 0.30 mmol), and  $\text{H}_2\text{O}$  (10 mL, 556 mmol) in the mole ratio 1:1.42:0.95:1754 was stirred briefly before heating to 120 °C for 72 h. The initial and final pH values were 2 and 1, respectively. Colorless blocks suitable for X-ray diffraction were isolated in 90% yield. IR (KBr pellet,  $\text{cm}^{-1}$ ): 2950(w), 2914(w), 2373(w), 1650(m), 1565(m), 1470(m), 1279(m), 1254(w), 1139(m), 1125(s), 1100(s), 985(s), 926(s), 770(s), 736(w), 566(s), 510(m). *Anal. Calc.* for  $\text{C}_{36}\text{H}_{38}\text{N}_4\text{O}_{12}\text{P}_4\text{Cd}$ : C, 45.2; H, 3.98; N, 5.86. Found: C, 44.2; H, 3.88; N, 5.71%.

#### 2.11. Synthesis of $[\text{Cd}(\text{o-phen})(1,2\text{-HO}_3\text{PC}_8\text{H}_8\text{PO}_3\text{H})]$ (**10**)

A solution of cadmium(II) nitrate tetrahydrate (0.098 g, 0.317 mmol), 1,10 phenanthroline (0.042 g, 0.23 mmol), o-xylene-diphosphonic acid (0.080 g, 0.30 mmol), and  $\text{H}_2\text{O}$  (10 mL, 556 mmol) in the mole ratio 1:0.73:0.95:1754 was stirred briefly before heating to 120 °C for 72 h. The initial and final pH values were 2 and 2, respectively. Colorless blocks suitable for X-ray diffraction were isolated in 70% yield. IR (KBr pellet,  $\text{cm}^{-1}$ ): 3447(w), 3054(w), 2362(w), 1635(w), 1557(w), 1519(w), 1448(w), 1424(m), 1278(m), 1231(m), 1164(w), 1132(s), 1024(s), 939(m), 890(s), 852(m), 789(m), 728(m), 542(m), 497(m). *Anal. Calc.* for  $\text{C}_{20}\text{H}_{18}\text{N}_2\text{O}_6\text{P}_2\text{Cd}$ : C, 43.1; H, 3.23; N, 5.03. Found: C, 42.6; H, 3.09; N, 4.85%.

#### 2.12. Synthesis of $[\text{Cd}(\text{o-phen})(1,3\text{-HO}_3\text{PC}_8\text{H}_8\text{PO}_3\text{H})]$ (**11**)

A solution of cadmium(II) nitrate tetrahydrate (0.098 g, 0.317 mmol), 1,10 phenanthroline (0.042 g, 0.23 mmol), m-xylene-diphosphonic acid (0.080 g, 0.30 mmol), and  $\text{H}_2\text{O}$  (10 mL, 556 mmol) in the mole ratio 1:0.73:0.95:1754 was stirred briefly before heating to 120 °C for 72 h. The initial and final pH values were 2 and 1, respectively. Colorless plates suitable for X-ray diffraction were isolated in 50% yield. IR (KBr pellet,  $\text{cm}^{-1}$ ): 3448(m), 3006(w), 2945(w), 2919(w), 1513(m), 1428(m), 1231(m), 1171(s), 1136(w), 1052(m), 1031(s), 923(s), 909(s), 850(m), 804(m), 728(s), 698(m), 523(s). *Anal. Calc.* for  $\text{C}_{20}\text{H}_{18}\text{N}_2\text{O}_6\text{P}_2\text{Cd}$ : C, 43.1; H, 3.23; N, 5.03. Found: C, 43.3; H, 3.68; N, 4.98%.

#### 2.13. Synthesis of $[\text{Cd}(\text{o-phen})(1,4\text{-HO}_3\text{PC}_8\text{H}_8\text{PO}_3\text{H})]$ (**12**)

A solution of cadmium(II) nitrate tetrahydrate (0.098 g, 0.317 mmol), 1,10 phenanthroline (0.042 g, 0.22 mmol), p-xylene-diphosphonic acid (0.080 g, 0.30 mmol), and  $\text{H}_2\text{O}$  (10 mL, 556 mmol) in the mole ratio 1:0.69:0.95:1754 was stirred briefly before heating to 120 °C for 72 h. The initial and final pH values were 2 and 1, respectively. Colorless blocks suitable for X-ray diffraction were isolated in 50% yield. IR (KBr pellet,  $\text{cm}^{-1}$ ): 3005(w), 2945(w), 2367(w), 1573(w), 1513(m), 1443(w), 1428(m), 1231(s), 1190(s), 1052(s), 1029(s), 923(s), 909(s), 862(m), 728(s), 697(s), 582(w), 575(s), 478(m). *Anal. Calc.* for  $\text{C}_{20}\text{H}_{18}\text{N}_2\text{O}_6\text{P}_2\text{Cd}$ : C, 43.1; H, 3.23; N, 5.03. Found: C, 43.4; H, 3.55; N, 5.11%.

#### 2.14. X-ray crystallography

Crystallographic data for all compounds were collected at low temperature (90 K) on a Bruker KAPPA APEX DUO diffractometer equipped with an APEX II CCD system using Mo  $\text{K}\alpha$  radiation ( $\lambda = 0.71073 \text{ \AA}$ ) [68,69]. The data were corrected for Lorentz and polarization effects [70], and adsorption corrections were made using SADABS [71]. The structures were solved by direct methods, and refinements were made using the SHELXTL [72] crystallographic software. After first locating all of the nonhydrogen atoms from the initial solution of each structure, the models were refined against  $F^2$  using first isotropic and then anisotropic thermal displacement parameters until the final value of  $\Delta/\sigma_{\text{max}}$  was less than 0.001. Hydrogen atoms were introduced in calculated positions and refined isotropically. Neutral atom scattering coefficients and anomalous dispersion corrections were taken from the *International Tables*, Vol. C. Crystallographic details for the structures of **1–12** are summarized in Table 1. Selected bond lengths and angles for the structures are given in Table S77. Images of the crystal structures were generated using CrystalMaker® [73].

#### 2.15. Thermogravimetric analyses

TGA data were collected on a TA instruments Q500 v6.7 Thermogravimetric Analyzer. Data was collected on samples that ranged between 5 and 10 mg, ramping the temperature at 10 °C/minute between ~25–800 °C.

#### 2.16. Luminescence studies

Spectra were obtained using a Photon Technologies International (Canada) QuantaMaster series spectrofluorometer modular system with an arc for steady state measurements and a pulsed Xenon arc lamp for measuring phosphorescence lifetimes based on a traveling wave gated PMT.

### 3. Results and discussion

#### 3.1. Syntheses

Hydrothermal methods, which were first applied for the synthesis of zeolites and metal phosphates [74,75], have been extended to the routine synthesis of metal oxides and organic-inorganic composite materials [76–79]. The technique, conventionally carried out in water at 120–250 °C at autogenous pressure, exploits “self-assembly” of a solid phase from soluble precursors at moderate temperatures. Product composition depends on a number of critical conditions, including pH of the medium, temperature and hence pressure, the presence of structure-directing cations, and the use of mineralizers.

Hydrothermal methods have been exploited for decades in the preparation of metal-diphosphonate materials with pillared layer structures, such as that of the prototypical pillared layer compound  $[\text{Cu}_2(\text{H}_2\text{O})_2(1,4\text{-O}_3\text{PC}_8\text{H}_8\text{PO}_3)]$  [80]. The introduction of auxiliary ligands, such as o-phenanthroline and 2,2'-bipyridyl, provides a method for reducing the overall dimensionality of the phase by blocking coordination sites at the metal and preventing structural expansion in one or more dimensions. The chain structures of compounds **1**, **2**· $\text{H}_2\text{O}$ , **5**· $\text{H}_2\text{O}$ , **7** and **11**, the layers associated with compounds **4**, **8** and **10**, and the one-dimensional substructures of the virtual two-dimensional materials **3** and **9** are characteristic examples of the use of simple auxiliary chelates in the design of lower dimensional materials. However, even in the presence of such chelating ancillary ligands, three-dimensional structures were observed for compounds **6**· $3\text{H}_2\text{O}$  and **12**, where the 1,

**Table 1**  
Summary of crystallographic data for structures of this study.

	(1)	(2)	(3)	(4)	(5)	(6)	(7)	(8)	(9)	(10)	(11)	(12)
	[Zn(H <sub>2</sub> O)(bpy)(1,2-HO <sub>3</sub> PC <sub>8</sub> H <sub>8</sub> PO <sub>3</sub> H)]	[Zn(H <sub>2</sub> O)(bpy)(1,2-HO <sub>3</sub> PC <sub>8</sub> H <sub>8</sub> PO <sub>3</sub> H)]·H <sub>2</sub> O	[Zn(o-phen)(1,2-HO <sub>3</sub> PC <sub>8</sub> H <sub>8</sub> PO <sub>3</sub> H)]·H <sub>2</sub> O	[Zn(o-phen)(1,2-HO <sub>3</sub> PC <sub>8</sub> H <sub>8</sub> PO <sub>3</sub> H)]·H <sub>2</sub> O	[Zn(o-phen)(1,2-HO <sub>3</sub> PC <sub>8</sub> H <sub>8</sub> PO <sub>3</sub> H)]·3H <sub>2</sub> O	[Zn <sub>2</sub> (o-phen) <sub>2</sub> (1,4-HO <sub>3</sub> PC <sub>8</sub> H <sub>8</sub> PO <sub>3</sub> H)]·3H <sub>2</sub> O	[Zn(tpyprz)(1,2-HO <sub>3</sub> PC <sub>8</sub> H <sub>8</sub> PO <sub>3</sub> H)]	[Cd(bpy)(1,3-HO <sub>3</sub> PC <sub>8</sub> H <sub>8</sub> PO <sub>3</sub> H)]	[Cd(bpy) <sub>2</sub> (1,4-HO <sub>3</sub> PC <sub>8</sub> H <sub>8</sub> PO <sub>3</sub> H)]	[Cd(o-phen)(1,2-HO <sub>3</sub> PC <sub>8</sub> H <sub>8</sub> PO <sub>3</sub> H)]	[Cd(o-phen)(1,3-HO <sub>3</sub> PC <sub>8</sub> H <sub>8</sub> PO <sub>3</sub> H)]	[Cd(o-phen)(1,4-HO <sub>3</sub> PC <sub>8</sub> H <sub>8</sub> PO <sub>3</sub> H)]
Empirical formula	C <sub>20</sub> H <sub>20</sub> N <sub>2</sub> O <sub>7</sub> P <sub>2</sub> Zn	C <sub>20</sub> H <sub>20</sub> N <sub>2</sub> O <sub>8</sub> P <sub>2</sub> Zn	C <sub>20</sub> H <sub>20</sub> N <sub>2</sub> O <sub>9</sub> P <sub>2</sub> Zn	C <sub>20</sub> H <sub>20</sub> N <sub>2</sub> O <sub>9</sub> P <sub>2</sub> Zn	C <sub>20</sub> H <sub>20</sub> N <sub>2</sub> O <sub>12</sub> P <sub>2</sub> Zn	C <sub>22</sub> H <sub>20</sub> N <sub>2</sub> O <sub>12</sub> P <sub>2</sub> Zn <sub>2</sub>	C <sub>20</sub> H <sub>20</sub> N <sub>3</sub> O <sub>7</sub> P <sub>2</sub> Zn	C <sub>20</sub> H <sub>20</sub> N <sub>3</sub> O <sub>7</sub> P <sub>2</sub> Zn	C <sub>20</sub> H <sub>20</sub> N <sub>4</sub> O <sub>7</sub> P <sub>2</sub> Zn	C <sub>20</sub> H <sub>20</sub> N <sub>2</sub> O <sub>9</sub> P <sub>2</sub> Zn	C <sub>20</sub> H <sub>20</sub> N <sub>2</sub> O <sub>9</sub> P <sub>2</sub> Zn	C <sub>20</sub> H <sub>20</sub> N <sub>2</sub> O <sub>9</sub> P <sub>2</sub> Zn
Formula weight	503.67	503.67	507.95	509.67	527.69	1828.64	717.90	532.68	954.98	556.70	556.70	556.70
Crystal system	orthorhombic	triclinic	monoclinic	monoclinic	monoclinic	triclinic	orthorhombic	triclinic	monoclinic	monoclinic	monoclinic	monoclinic
Space group	P2 <sub>1</sub> (1)2(1)	P1	C2/c	P2 <sub>1</sub> /n	C2/c	P1	Pca2(1)	P1	C2/c	P2(1)/n	P2(1)/c	C2/c
a (Å)	9.7554(10)	8.7090(8)	18.008(3)	10.4437(17)	21.852(2)	11.4878(13)	19.987(4)	7.7530(8)	18.054(3)	10.558(2)	10.9168(18)	21.403(9)
b (Å)	14.3904(14)	10.6717(10)	24.449(3)	14.613(2)	9.2934(11)	11.9511(14)	16.880(3)	10.9310(11)	24.956(4)	14.728(3)	23.782(4)	12.239(3)
c (Å)	14.7968(14)	11.4670(11)	8.7840(12)	12.548(2)	22.266(2)	15.1124(18)	8.9332(18)	11.1915(11)	8.7687(13)	12.647(3)	7.6752(13)	7.687(2)
α (°)	90.00	93.428(2)	90.00	90.00	90.00	81.059(2)	90.00	96.747(2)	90.00	90.00	90.00	90.00
β (°)	90.00	96.191(2)	102.756(3)	104.566(3)	110.313(2)	78.308(2)	90.00	90.948(2)	102.471(3)	104.631(5)	95.977(4)	98.983(10)
γ (°)	90.00	109.753(2)	90.00	90.00	90.00	61.526(2)	90.00	95.753(2)	90.00	90.00	90.00	90.00
V (Å <sup>3</sup> )	2077.2(4)	991.89(16)	3772.0(9)	1853.5(5)	4239.3(8)	1781.8(4)	3014.0(10)	936.76(16)	3857.6(10)	1902.7(6)	1981.8(6)	1989.9(11)
Z	4	2	4	4	8	1	4	2	4	4	4	4
D <sub>calc</sub> (g cm <sup>-3</sup> )	1.611	1.686	1.599	1.826	1.654	1.704	1.582	1.889	1.644	1.943	1.866	1.859
μ (mm <sup>-1</sup> )	1.380	1.445	0.891	1.544	1.357	1.550	0.979	1.378	0.801	1.361	1.307	1.302
T (K)	90(2)	90(2)	90(2)	90(2)	90(2)	90(2)	90(2)	90(2)	90(2)	90(2)	90(2)	90(2)
Wavelength	0.71073	0.71073	0.71073	0.71073	0.71073	0.71073	0.71073	0.71073	0.71073	0.71073	0.71073	0.71073
R <sub>1</sub> <sup>a</sup>	0.0185	0.0229	0.0255	0.0303	0.0287	0.0263	0.0144	0.0144	0.0207	0.0186	0.0257	0.0279
wR <sub>2</sub> <sup>b</sup>	0.0470	0.0628	0.0674	0.0650	0.0756	0.0740	0.0828	0.0398	0.0564	0.0473	0.0613	0.0653

$$^a R_1 = \sum |F_o| - |F_c| / \sum |F_o|$$

$$^b wR_2 = \{ \sum [w(F_o^2 - F_c^2)^2] / \sum [w(F_o^2)] \}^{1/2}$$

4-xylyldiphosphonate ligand provides sufficient spatial extension to encapsulate the chelating organonitrogen ligands within the framework void spaces.

Such naïve design principles also did not extend to the chemistry of the Zn(II)/tpyprz/xylyl-diphosphonate system. Our expectation was that the dipodal tpyprz would bridge metal sites of zinc-diphosphonate chains to expand the structure into two-dimensions. However, the tpyprz coordinates to a single metal site so as to decorate the surface of the chain, projecting one uncoordinated pyrazine face and two uncoordinated pyridyl groups into the extra-linkage domain. Similar results were observed for the previously reported Mn(II), Co(II) and Ni(II) complexes of the xylyldiphosphonates when tpyprz was incorporated into the chain [81].

It is also noteworthy that xylyl-diphosphonate ligands may adopt a variety of protonated forms, in addition to the more common fully deprotonated tetranegative anion {O<sub>3</sub>P-R-PO<sub>3</sub>}<sup>4-</sup>. Under the conditions of this study, the symmetrically protonated form {HO<sub>3</sub>PC<sub>8</sub>H<sub>8</sub>PO<sub>3</sub>H}<sup>2-</sup> predominates.

The infrared spectra of compounds 1–12 exhibit a pattern of two or three medium to strong bands in the 1000–1200 cm<sup>-1</sup> range attributed to ν(P–O) of the phosphonate ligands. In addition, compounds 2·H<sub>2</sub>O, 5·H<sub>2</sub>O and 6·3H<sub>2</sub>O exhibit an intense broad band at ca. 3100 cm<sup>-1</sup> assigned to ν(O–H) of the coordinated water molecules.

### 3.2. Descriptions of the structures of this study

As shown in Fig. 1, the structure of [Zn(bpy)(H<sub>2</sub>O)(1,2-HO<sub>3</sub>PC<sub>8</sub>H<sub>8</sub>PO<sub>3</sub>H)] (1) is one-dimensional with the {Zn(II)-diphosphonate}<sub>n</sub> segment describing a shallow helix. The zinc sites exhibit distorted trigonal bipyramidal geometry through bonding to a nitrogen donor of the bpy chelate and oxygen donors from two diphosphonate ligands in the equatorial plane and an aqua oxygen and the second bipyridyl nitrogen in the axial positions. Each diphosphonate ligand in turn bridges two zinc centers through sharing of a single oxygen donor at each {-PO<sub>3</sub>} terminus of the ligand. Each {-PO<sub>3</sub>} terminus is protonated at a single oxygen site, readily located on the final difference Fourier and also apparent from P–O and P–O(H) average distances of 1.514(1) and 1.567(1) Å, respectively.

It is noteworthy that the 1,2-xylyldiphosphonate ligand with Mn(II) and bpy yields the previously described two-dimensional material [Mn(bpy)(1,2-HO<sub>3</sub>PC<sub>8</sub>H<sub>8</sub>PO<sub>3</sub>H)] where the square pyramidal Mn sites are paired in the characteristic di-μ(O,O') phosphonate bridged binuclear units [81].

When o-phenanthroline is substituted for bpy, the two-dimensional [Zn(o-phen)(1,2-HO<sub>3</sub>PC<sub>8</sub>H<sub>8</sub>PO<sub>3</sub>H)] (4) is obtained (Fig. 2). The structure is constructed from the afore-mentioned units of di-μ(O,O') phosphonate bridging two metal square pyramids in a {Zn<sub>2</sub>P<sub>2</sub>O<sub>4</sub>} eight-membered ring. A secondary building unit consisting of two zinc square pyramids and four phosphorous tetrahedra is connected to four adjacent {Zn<sub>2</sub>(o-phen)<sub>2</sub>(RPO<sub>3</sub>H)<sub>4</sub>} clusters through the xylyl spacers to provide the two-dimensional network structure.

The basal plane of each Zn(II) site is defined by the oxygen donors of the two bridging diphosphonate tetrahedra and the nitrogen donors of the o-phen chelate. The apical site is occupied by an oxygen donor from one terminus of a diphosphonate ligand linking to an adjacent binuclear zinc site of the layer. Thus, each diphosphonate ligand uses one terminus in bridging the metal sites of one cluster while the second bonds to a single metal site of an adjacent cluster. The linkage pattern produces intralamellar cavities of approximate dimensions 12.7 × 9.4 Å whose boundaries are defined by four {Zn<sub>2</sub>(o-phen)<sub>2</sub>(RPO<sub>3</sub>H)<sub>4</sub>} clusters. The two-dimensional structure of 4 is isomorphous with the previously described [Mn(bpy)(1,2-HO<sub>3</sub>PC<sub>8</sub>H<sub>8</sub>PO<sub>3</sub>H)], [Mn(o-phen)(1,2-HO<sub>3</sub>

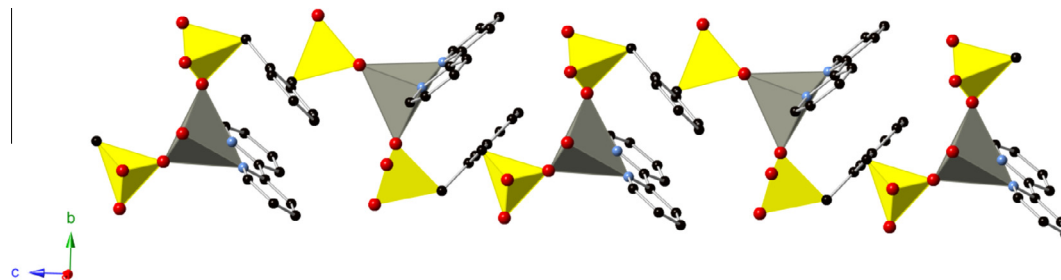


**Fig. 1.** A mixed polyhedral and ball-and-stick representation of the structure of  $[\text{Zn}(\text{H}_2\text{O})(\text{bpy})(1,2\text{-HO}_3\text{PC}_8\text{H}_8\text{PO}_3\text{H})]$  (**1**). Color scheme: Zn, grey polyhedra; P, yellow polyhedra; oxygen, red spheres, nitrogen, light blue spheres; carbon, black spheres. This scheme is used throughout. (For interpretation of the references to colour in this figure legend, the reader is referred to the web version of this article.)

$\text{PC}_8\text{H}_8\text{PO}_3\text{H})]$  and  $[\text{Co}(\text{o-phen})(1,2\text{-HO}_3\text{PC}_8\text{H}_8\text{PO}_3\text{H})]$ . This recurrent network structure is also observed for the Cd(II) analogue  $[\text{Cd}(\text{o-phen})(1,2\text{-HO}_3\text{PC}_8\text{H}_8\text{PO}_3\text{H})]$  (**10**).

In common with structures of this general type, the distances from the metal to the basal oxygen donors are significantly shorter than the metal-apical oxygen distances:  $\text{Zn-O}_{\text{basal}}(\text{ave}): 1.977(2) \text{ \AA}$ ;  $\text{Zn-O}_{\text{apical}}: 2.057(2) \text{ \AA}$ ;  $\text{Cd-O}_{\text{basal}}(\text{ave}): 2.162(1) \text{ \AA}$ ;  $\text{Cd-O}_{\text{apical}}: 2.219(1) \text{ \AA}$ . The protonation sites on the phosphate oxygen atoms are again revealed in the bond distances: P–O (ave):  $1.512(2) \text{ \AA}$  (**4**) and  $1.506(2) \text{ \AA}$  (**10**); P–O(H) (ave):  $1.578(2) \text{ \AA}$  (**4**) and  $1.571(2) \text{ \AA}$  (**10**).

While compound **2**·H<sub>2</sub>O,  $[\text{Zn}(\text{bpy})(1,3\text{-HO}_3\text{PC}_8\text{H}_8\text{PO}_3\text{H})]\cdot\text{H}_2\text{O}$  (**2**·H<sub>2</sub>O) is one-dimensional, the structure is quite distinct from that of **1**. As shown in Fig. 3, the building unit in this case is the  $\{\text{M}_2\text{P}_2\text{O}_4\}$  ring of di- $\mu(\text{O},\text{O}')$  phosphonate groups bridging metal square pyramids. This linkage provides the  $\{\text{Zn}_2(\text{o-phen})_2(\text{RPO}_3\text{H})_4\}$  cluster building block, each of which is linked to two adjacent clusters of the chain. Each diphosphonate ligand provides two oxygen atoms of one  $\{-\text{PO}_3\text{H}\}$  terminus to bridge the zinc sites of a cluster unit, while one oxygen donor of the second terminus bonds to a metal site of an adjacent cluster.

The zinc geometry is defined by the nitrogen donors of the chelate and two oxygen donors in the basal plane while an oxygen from a third diphosphonate ligand occupies the apical position. The common bond length pattern is observed:  $\text{Zn-O}_{\text{basal}}: 1.953(1) \text{ \AA}$ ;  $\text{Zn-O}_{\text{apical}}: 2.035(1) \text{ \AA}$ . The protonation sites are again obvious with P–O and P–O(H) average distances of  $1.512(2)$  and  $1.576(2) \text{ \AA}$ , respectively.

The structures of the o-phen derivatives  $[\text{Zn}(\text{o-phen})(1,3\text{-HO}_3\text{PC}_8\text{H}_8\text{PO}_3\text{H})]\cdot\text{H}_2\text{O}$  (**5**·H<sub>2</sub>O) and  $[\text{Cd}(\text{o-phen})(1,3\text{-HO}_3\text{PC}_8\text{H}_8\text{PO}_3\text{H})]$  (**11**) are similar to that of compound **2**·H<sub>2</sub>O. A nearly identical double chain structure is observed with projecting o-phenanthroline ligands replacing the bpy ligands of **2**·H<sub>2</sub>O. The usual trends in bond distances are observed, as shown in Table S77.

Low dimensional structures may be designed by introducing coligands of higher denticity, such as tetra-2-pyridinylpyrazine, and the one-dimensional theme is observed for  $[\text{Zn}(\text{tpyprz})(1,2\text{-HO}_3\text{PC}_8\text{H}_8\text{PO}_3\text{H})]$  (**7**), shown in Fig. 4. The structure consists of distorted trigonal bipyramidal  $\{\text{ZnN}_3\text{O}_2\}$  sites linked through the xylyldiphosphonate ligands. The equatorial plane is defined by oxygen donors from  $\{-\text{PO}_3\text{H}\}$  groups of two xylyldiphosphonate ligands and the nitrogen donor of the pyrazine group. The axial positions are occupied by the pyridyl nitrogen donors of one side of the tpyprz ligands. In common with the previously reported one-dimensional structure  $[\text{M}(\text{tpyprz})(1,2\text{-HO}_3\text{PC}_8\text{H}_8\text{PO}_3\text{H})]$  ( $\text{M} = \text{Co}, \text{Ni}$ ), the other pyrazine nitrogen and two pyridyl arms of the tpyprz ligand are uncoordinated. However, the metal sites of the Co and Ni derivatives adopt  $\{\text{MO}_3\text{N}_3\}$  distorted octahedral coordination geometries that result in the common  $\{\text{M}_2(\text{tpyprz})_2(\text{RPO}_3\text{H})_2\}$  cluster as the secondary building unit.

The isomorphous 1,4-xylyldiphosphonate derivatives  $[\text{M}(\text{bpy})_2(1,4\text{-H}_2\text{O}_3\text{PC}_8\text{H}_8\text{PO}_3\text{H}_2)(1,4\text{-HO}_3\text{PC}_8\text{H}_8\text{PO}_3\text{H})]$  ( $\text{M} = \text{Zn}$  (**3**),  $\text{Cd}$  (**9**)) exhibit the unusual, but apparently common, virtual two-dimensional network structure of Fig. 5. The structures are similar to those previously reported for  $[\text{M}(\text{N}\sim\text{N})_2(1,4\text{-H}_2\text{O}_3\text{PC}_8\text{H}_8\text{PO}_3\text{H}_2)(1,4\text{-HO}_3\text{PC}_8\text{H}_8\text{PO}_3\text{H})]$  ( $\text{M} = \text{Mn}, \text{N}\sim\text{N} = \text{bpy}$ ;  $\text{M} = \text{Co}, \text{Ni}$ , and  $\text{N}\sim\text{N} = \text{o-phen}$ ). The structure is constructed from  $\{\text{M}(\text{N}\sim\text{N})_2(1,4\text{-HO}_3\text{PC}_8\text{H}_8\text{PO}_3\text{H})\}_n^{2n+}$  chains that are distinct from the one-dimensional motifs adopted by compounds **1**, **2**·H<sub>2</sub>O, **8** and **11** of this study. In the case of **3** and **9**, each metal bonds to two bpy or o-phen ligands and to two fully protonated diphosphonate ligands,  $\text{H}_2\text{O}_3\text{PC}_8\text{H}_8\text{PO}_3\text{H}_2$ , to give *cis*- $\{\text{MO}_2\text{N}_4\}$  coordination geometry. Adjacent metal octahedra of the chain are linked through the 1,4-xylyldiphosphonic acid ligands, each bonding to one metal site through one oxygen of each terminus. The remaining oxygen atoms are protonated, such that the one-dimensional substructure is positively charged,  $\{\text{M}(\text{N}\sim\text{N})_2(1,4\text{-H}_2\text{O}_3\text{PC}_8\text{H}_8\text{PO}_3\text{H}_2)\}_n^{2n+}$ .

The structure expands into a virtual two-dimensional network through strong multipoint hydrogen-bonding between the P–O(H) groups of the chains and the unprotonated oxygen atoms of the associated but uncoordinated  $\{\text{HO}_3\text{PC}_8\text{H}_8\text{PO}_3\text{H}\}^{2-}$  anions. The hydrogen-bonding interactions, shown in Fig. 5b, result in a two-dimensional network of cationic chains linked through diphosphonate anions. The  $\{\text{M}(\text{N}\sim\text{N})_2\}^{2+}$  groups of the layers project above and below the plane into the interlamellar domain. These projecting units from adjacent layers interdigitate to produce a dense structure with minimal void space.

The protonation sites of **3** and **9** are revealed by the appearance of peaks at appropriate locations in the Fourier maps and by the usual trends in P–O and P–O(H) bond distances. As shown in Table S77, the metrical parameters are unexceptional.

The two-dimensional theme is recurrent in the structure of  $[\text{Cd}(\text{bpy})(1,3\text{-HO}_3\text{PC}_8\text{H}_8\text{PO}_3\text{H})]$  (**8**), shown in Fig. 6. However, the juxtaposition of the common  $\{\text{M}_2(\text{N}\sim\text{N})(\text{RPO}_3\text{H})_2\}$  clusters in **8** is quite distinct from that of network structures of **4** and **10** of this study. Rather than the isolated clusters with radiating xylyl tethering arms of the latter, **8** exhibits chains of  $\{\text{Cd}_2(\text{N}\sim\text{N})(\text{RPO}_3\text{H})_2\}$  units running parallel to the *a* or *c* axis, respectively. Adjacent chains are linked through the xylyl tethers of the diphosphonate ligands to establish the two-dimensional connectivity.

The Cd(II) sites of **8** exhibit trigonally distorted  $\{\text{CdO}_4\text{N}_2\}$  octahedral geometries. As illustrated by compound **8**, the  $\{\text{CdO}_3\}$  face of the polyhedra exhibits an average bond distance of  $2.246(1) \text{ \AA}$  while the  $\{\text{MON}_2\}$  face has an average bond distance of  $2.352(1) \text{ \AA}$ . Once again, the protonation sites are apparent from the P–O and P–O(H) distances.

Curiously, there is a single example of a three-dimensional structure for the Zn(II) series,  $[\text{Zn}_4(\text{o-phen})_4(1,4\text{-HO}_3\text{PC}_8\text{H}_8\text{PO}_3)_2(1,4\text{-HO}_3\text{PC}_8\text{H}_8\text{PO}_3\text{H})]\cdot\text{H}_2\text{O}$  (**6**·H<sub>2</sub>O), shown in Fig. 7. The structure is constructed from the common  $\{\text{Zn}_2(\text{o-phen})_2(\text{RPO}_3)_2\}$  subunits

linked into a one-dimensional chain through  $\{RPO_3\}$  tetrahedra. These chains are distinct from those observed for **8** and **12** which consist of  $\{M_2(N\sim N)(RPO_3H)_2\}$  units linked by two  $\{RPO_3H\}$  tetrahedra at each metal site to the two adjacent binuclear building units of the chain. In effect, each  $M(II)$  site shares a vertex with four  $\{RPO_3H\}$  tetrahedra. In the case of compound **6**· $H_2O$ , each  $\{Zn_2(o\text{-phen})_2(RPO_3H_x)_2\}$  unit is linked to adjacent clusters through a single  $\{RPO_3\}$  group, such that each  $Zn(II)$  site is associated with three phosphonate tetrahedra rather than four.

The  $\{Zn_2(o\text{-phen})_2(RPO_3H_x)_n\}$  chains run parallel to the crystallographic  $c$ -axis and the xyllyl tethers of the diphosphonate ligands radiate outward along the  $a$  and  $b$  directions connecting each chain to four adjacent chains. The xyllyl tethers provide sufficient spacing between chains to generate channels of rhombic profile of dimensions 11.5 by 8.4 Å, accommodating the  $o\text{-phen}$  groups that project outward from the chain axes.

The zinc sites exhibit distorted square pyramidal  $\{ZnO_3N_2\}$  geometry with the basal plane occupied by the  $o\text{-phen}$  nitrogen

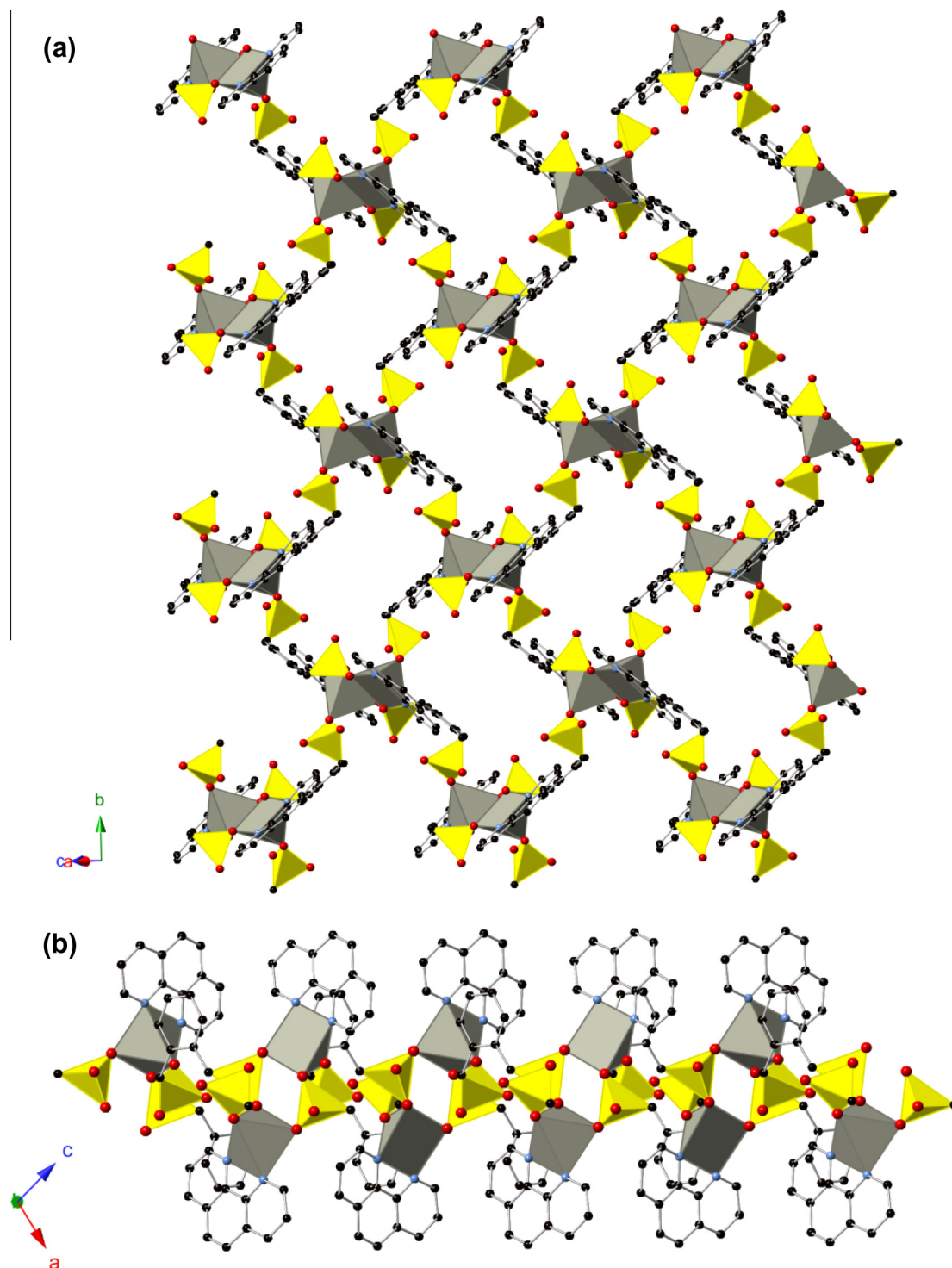


**Fig. 2.** (a) A view of the two-dimensional structure of  $[Zn(o\text{-phen})(1,2\text{-HO}_3\text{PC}_8\text{H}_8\text{PO}_3\text{H})]$  (**4**); (b) a view of the structure in the  $ac$  plane. The structure of  $[Cd(o\text{-phen})(1,2\text{-HO}_3\text{PC}_8\text{H}_8\text{PO}_3\text{H})]$  (**10**) is isomorphous.

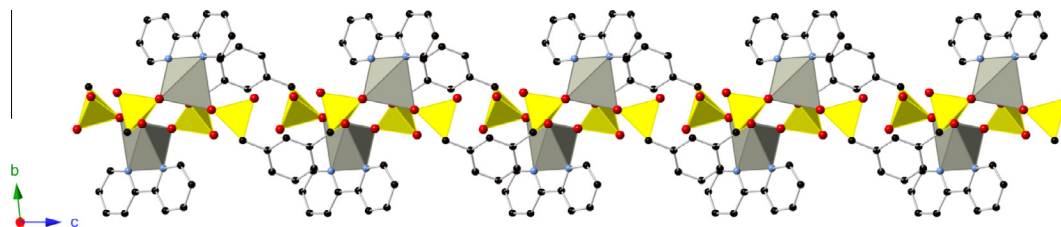


**Fig. 3.** A view of the one-dimensional structure of  $[\text{Zn}(\text{bpy})(1,3\text{-HO}_3\text{PC}_8\text{H}_8\text{PO}_3\text{H})]\cdot\text{H}_2\text{O}$  ( $2\cdot\text{H}_2\text{O}$ ). The structures of  $[\text{M}(\text{o-phen})(1,3\text{-HO}_3\text{PC}_8\text{H}_8\text{PO}_3\text{H})]$  ( $\text{M} = \text{Zn}$  (**5**) and  $\text{Cd}$  (**11**)) exhibit similar connectivities.

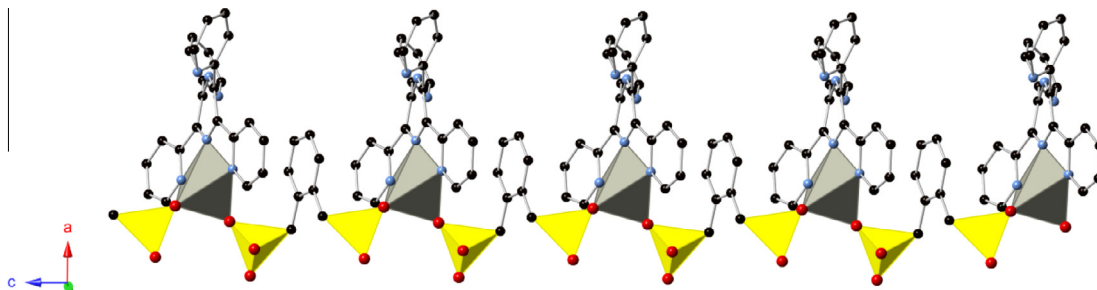


**Fig. 4.** A view of the one-dimensional structure of  $[\text{Zn}(\text{tpyprz})(1,2\text{-HO}_3\text{PC}_8\text{H}_8\text{PO}_3\text{H})]$  (**7**).

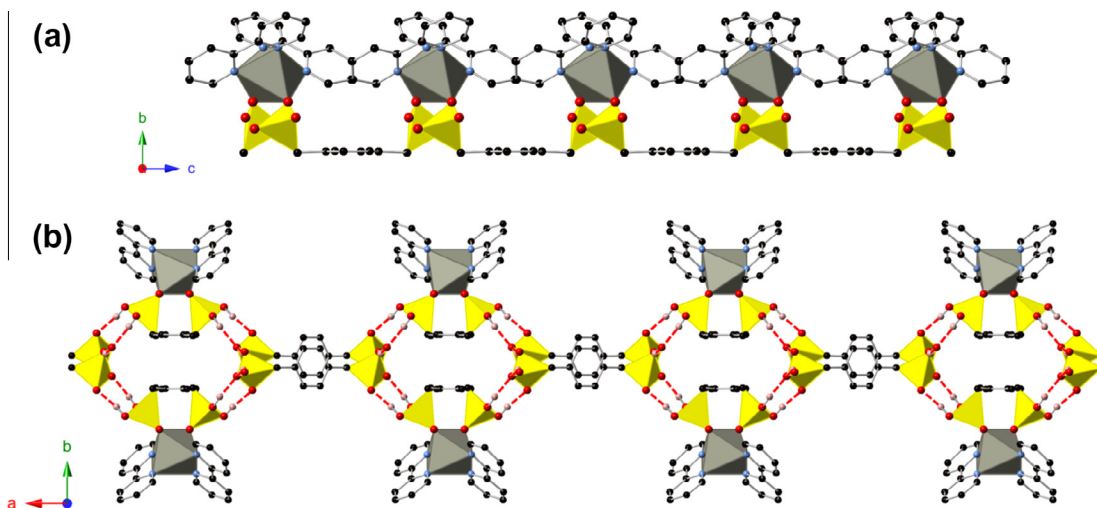


**Fig. 5.** (a) A view of the one-dimensional substructure of  $[\text{Zn}(\text{bpy})_2(1,4\text{-H}_2\text{O}_3\text{PC}_8\text{H}_8\text{PO}_3\text{H}_2)(1,4\text{-HO}_3\text{PC}_8\text{H}_8\text{PO}_3\text{H})]$  (**3**) in the  $bc$  plane; (b) a view of the structure of **3** in the  $ab$  plane, showing the hydrogen bonding between  $\{\text{Zn}_2(\text{o-phen})_2(\text{RPO}_3\text{H})_2\}^{2n+}$  chains and the  $\{\text{HO}_3\text{PC}_8\text{H}_8\text{PO}_3\text{H}\}^{2-}$  anions. The structure of  $[\text{Cd}(\text{bpy})_2(1,4\text{-H}_2\text{O}_3\text{PC}_8\text{H}_8\text{PO}_3\text{H}_2)(1,4\text{-HO}_3\text{PC}_8\text{H}_8\text{PO}_3\text{H})]$  (**9**) is isomorphous. Color scheme: Cd, blue polyhedra; other atoms as above. (For interpretation of the references to colour in this figure legend, the reader is referred to the web version of this article.)

donors and two phosphonate oxygen atoms; the oxygen donor from a third phosphonate group adopts the apical position. There are two distinct xylyldiphosphonate ligands. The first is in the symmetrically singly protonated form  $\{\text{HO}_3\text{PC}_8\text{H}_8\text{PO}_3\text{H}\}^{2-}$  which bridges two zinc sites of a  $\{\text{Zn}_2(\text{o-phen})_2(\text{RPO}_3\text{H})_2\}$  cluster at either terminus and is aligned parallel to the  $b$  axis. The second xylyldiphosphonate ligand employs one terminus as a bridge within a  $\{\text{Zn}_2(\text{o-phen})_2(\text{RPO}_3\text{H})_2\}$  cluster with the second terminus present as a fully deprotonated  $\{\text{RPO}_3\}^{2-}$  unit bridging two  $\{\text{Zn}_2(\text{o-phen})_2(\text{RPO}_3\text{H})_2\}$  clusters of an adjacent chain. The P–O and P–O(H) bond lengths for the three  $\{\text{RPO}_3\text{H}\}$  termini of the two ligands are 1.507(2) Å (ave) and 1.564(2) Å, respectively, while the P–O distances for the fully deprotonated unit are 1.516(2) Å for

the pendant oxo-group and 1.541(2) and 1.542(2) Å for the metal ligated oxygen atoms.

The second example of a three-dimensional structure is provided by compound **12**,  $[\text{Cd}(\text{o-phen})(1,4\text{-HO}_3\text{PC}_8\text{H}_8\text{PO}_3\text{H})]$  (**12**). Once again, the common  $\{\text{M}_2(\text{N}\sim\text{N})_2(\text{HO}_3\text{PR})_2\}$  secondary building unit is encountered. As shown in Fig. 8, these clusters fuse into chains in a fashion reminiscent of the structure of compound **8**. However, in this case, each chain is linked through the 1,4-diphosphonate ligand to four adjacent chains, rather than two as for **8**, to provide expansion into the third dimension. An unusual feature of the structure is the large cavities running parallel to the  $c$ -axis, formed by four  $\{\text{M}_2(\text{HO}_3\text{PR})_2\}$  clusters and the four bridging 1,4-xylyl groups, which are occupied by the  $\text{o-phen}$  ligands.

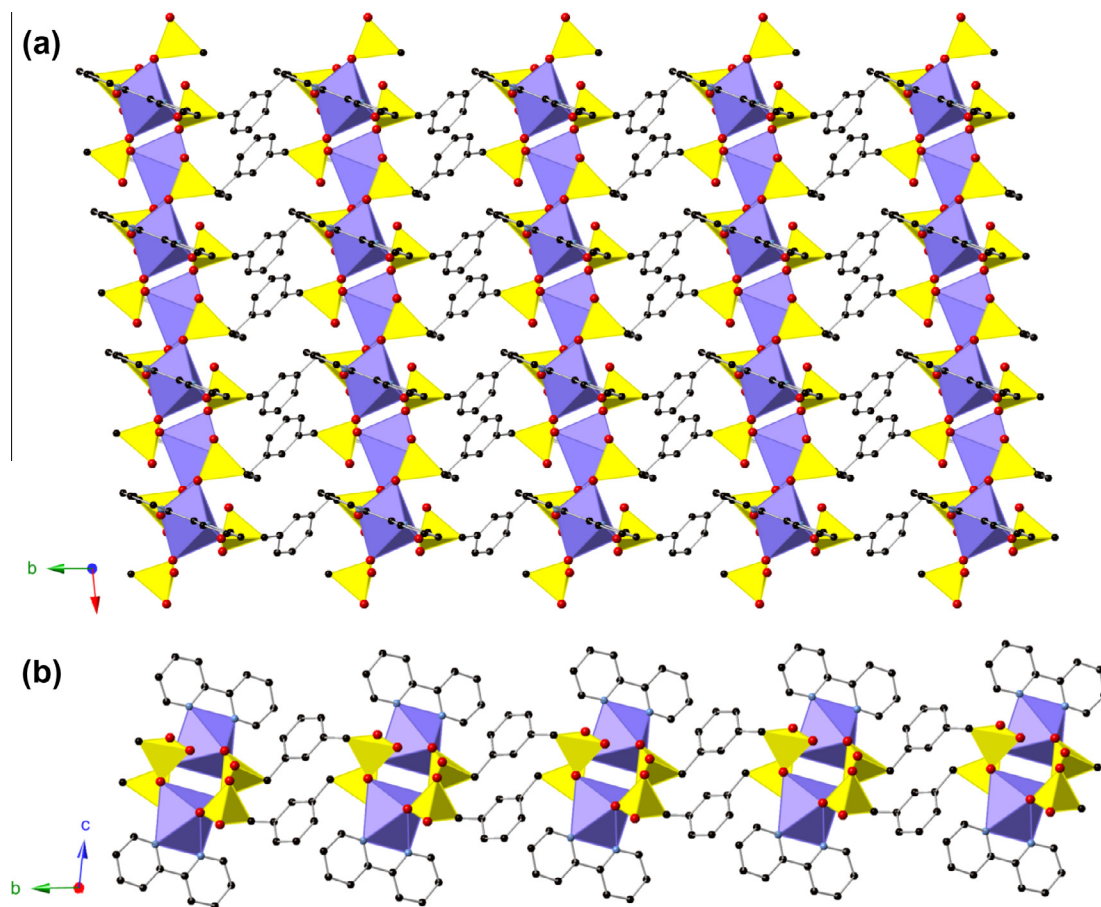


Fig. 6. (a) A view of the two-dimensional structure of  $[\text{Cd}(\text{bpy})(1,3\text{-HO}_3\text{PC}_8\text{H}_8\text{PO}_3\text{H})]$  (**8**) in the  $ab$  plane; (b) the structure shown in the  $bc$  plane.

Consequently, the *o*-phen groups, which decorate the surfaces of the layers in the previously described two-dimensional series, are incorporated into organic–inorganic capsules within the three-dimensional framework of **12**.

### 3.3. Structural trends and observations

The consequences of incorporation of ancillary chelating ligands are evident in the structures of this study and those of the Mn(II), Co(II), Ni(II) and Cu(II) series previously described [77,78]. The expectation that occupation of coordination sites on the metal centers by the organonitrogen chelates would effect reduction of the overall dimensionality of the materials has been realized. In the absence of this secondary chelating ligand, pillared layer structures are the rule in general and specifically in the xylyldiphosphonate derivative  $[\text{Cu}_2(\text{H}_2\text{O})_2(1,4\text{-O}_3\text{PC}_8\text{H}_8\text{PO}_3)]$  [82]. However, as noted in Table 2, in the presence of the secondary ligands, there are only three instances of three-dimensional structures  $[\text{M}(\text{o-phen})(1,4\text{-xdpH}_2)]$  ( $\text{M} = \text{Co}, \text{Cd}$ ) and the unusual  $[\text{Zn}_4(\text{o-phen})_4(1,4\text{-xdpH}_2)(1,4\text{-xdpH}_3)_2]$ , which do not exhibit the prototypical pillared layer structure but one derived from the recurrent  $\{\text{M}_2(\text{RPO}_3)_2\}$  building unit ( $\text{xdpH}_2 = \text{xylyldiphosphonic acid}$ ) shown in Fig. 9.

It is noteworthy that the multidentate capability of diphosphonate ligands favors the formation of extended structures and often of insoluble polymeric materials [58]. Molecular or zero-dimensional phosphonates are relatively rare [83]. Curiously, the molecular species encountered in our studies are exclusively Cu(II) species, although the reactions conditions were similar for the preparation of all phases described in the table. The molecular

species also reveal the pronounced tendency of the copper in these compounds to adopt ‘4 + 1’ axially elongated square pyramidal geometry, a common structural feature of  $d^9$ -Jahn–Teller distorted Cu(II) complexes.

The denticity of the secondary ligand also results in dramatic structural consequences. The *tpyprz* ligand was introduced as a tridentate, binucleating ligand in the naive expectation that this would provide expansion into three-dimensional structures. However, only molecular  $[\text{Cu}_2(\text{tpyprz})(1,2\text{-xdpH}_2)_2]$  and  $[\text{Cu}_4\text{Cl}_4(\text{tpyprz})_2(1,4\text{-xdpH}_3)_2]\text{Cl}_2$ , and one-dimensional,  $[\text{M}(\text{tpyprz})(1,2\text{-xdpH}_2)]$  ( $\text{M} = \text{Co}, \text{Ni}, \text{Zn}$ ) and  $[\text{Ni}_2(\text{tpyprz})(1,4\text{-xdpH}_2)]$  structures were observed. In all cases but that of  $[\text{Ni}_2(\text{tpyprz})(1,4\text{-xdpH}_2)]$ , the *tpyprz* ligand binds to a single site, projecting two pendant pyridyl groups.

The coordination preferences of the metals are also contributory structural determinants. For example, the one-dimensional structures of  $[\text{Cu}(\text{bpy})(1,3\text{-xdpH}_2)]$  and  $[\text{Cu}(\text{o-phen})(1,3\text{-xdpH}_2)]$  are similar to those of Zn(II) and Cd(II) analogues  $[\text{M}(\text{N}\sim\text{N})(1,3\text{-xdpH}_2)]$  ( $\text{N}\sim\text{N} = \text{bpy}$  and *o-phen*) with  $\{\text{MN}_2\text{O}_3\}$  square pyramidal coordination geometries and quite distinct from the two-dimensional series of 1,3-*xdpH*<sub>2</sub> analogues,  $[\text{M}(\text{N}\sim\text{N})(1,3\text{-xdpH}_2)]$  ( $\text{M} = \text{Mn}, \text{Co}, \text{Ni}$ ;  $\text{N}\sim\text{N} = \text{bpy}, \text{o-phen}$ ), where octahedral  $\{\text{MN}_2\text{O}_4\}$  coordination is observed.

While there is a predominance of structures exhibiting square pyramidal coordination geometries, six coordination is also common. For example, the Cd(II) derivatives  $[\text{Cd}(\text{bpy})(1,2\text{-xdpH}_2)]$  and  $[\text{Cd}(\text{o-phen})(1,4\text{-xdpH}_2)]$  exhibit  $\{\text{CdN}_2\text{O}_4\}$  octahedral geometry, whose building units,  $\{\text{Cd}_2(\text{RPO}_3)_2\}$  rings fused into one-dimensional chains, are similar to those of the two-dimensional phases  $[\text{M}(\text{N}\sim\text{N})(1,3\text{-xdpH}_2)]$  ( $\text{M} = \text{Mn}, \text{Co}, \text{Ni}$  and  $\text{N}\sim\text{N} = \text{bpy}$  and

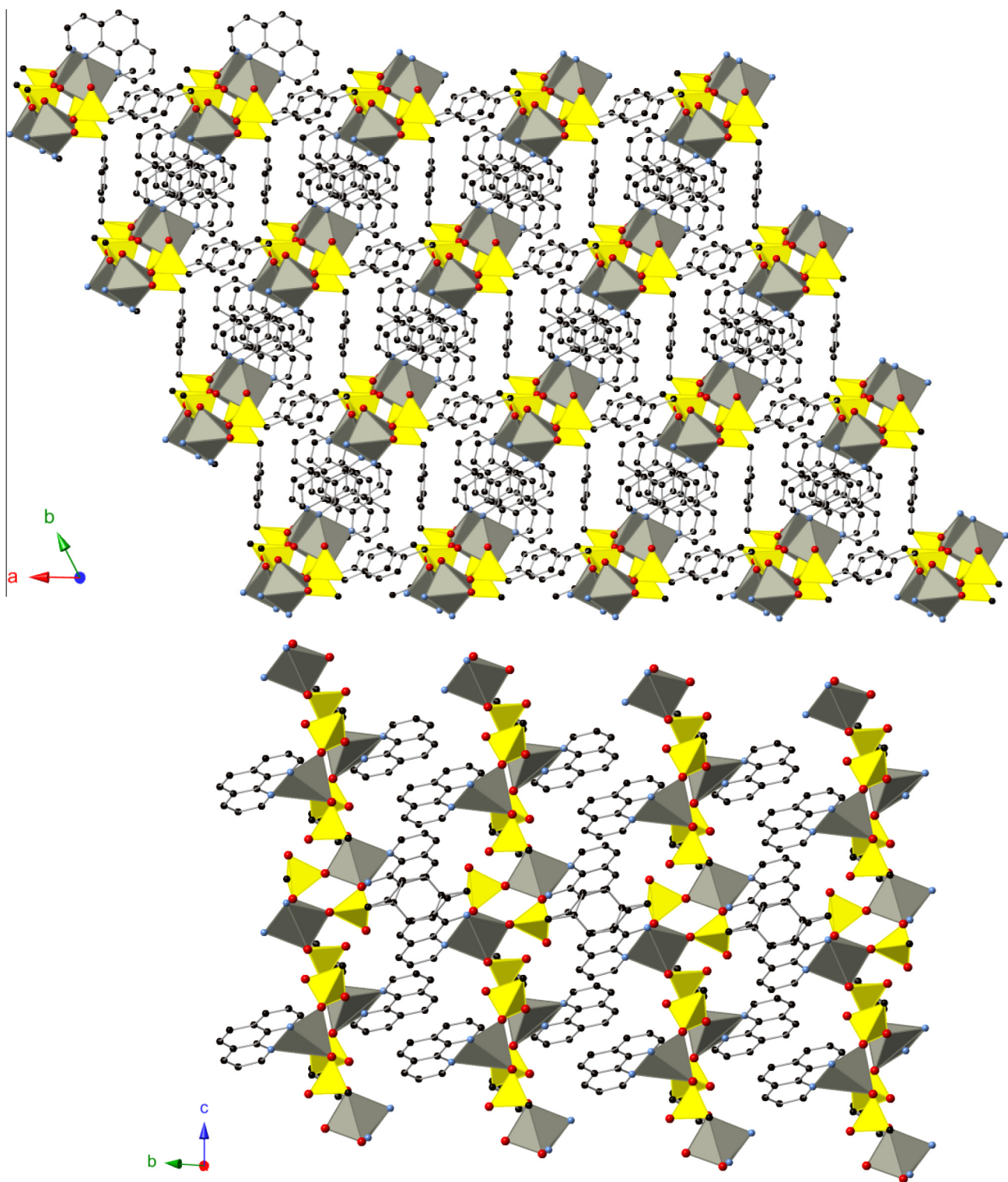


**Fig. 7.** (a) A view of the three-dimensional structure of  $[\text{Zn}_4(\text{o-phen})_4(1,4\text{-HO}_3\text{PC}_8\text{H}_8\text{PO}_3)_2(1,4\text{-HO}_3\text{PC}_8\text{H}_8\text{PO}_3\text{H})]\cdot 3\text{H}_2\text{O}$  (**6** $\cdot\text{H}_2\text{O}$ ) in the  $ab$  plane; (b) a view of the structure of **6** in the  $bc$  plane showing the  $[\text{Zn}_2(\text{o-phen})_2(\text{RPO}_3\text{H}_x)_3]_n$  one-dimensional substructures and the linkage through the xylidyl chains.

*o-phen*) where a different xylidyl ligand is employed. Thus, the  $[\text{Cd}(\text{bpy})(1,2\text{-xdpH}_2)]$  and  $[\text{M}(\text{N}\sim\text{N})(1,3\text{-xdpH}_2)]$  series of compounds exhibit similar overall two-dimensional connectivities despite the incorporation of 1,2- or 1-3-xylidyl diphosphonate ligands. In general, this is not the case, as the relative locations of the methylenephosphonate groups on the ligand phenyl ring result in distinctive structural types. Consequently, the two-dimensional

structures  $[\text{M}(\text{N}\sim\text{N})(1,2\text{-xdpH}_2)]$  ( $\text{M} = \text{Mn, Co, Cu, Zn, Cd}$ ) are quite distinct from the network structures  $[\text{M}(\text{N}\sim\text{N})(1,3\text{-xdpH}_2)]$  ( $\text{M} = \text{Mn, Co, Ni}$ ) and from the virtual two-dimensional structures of the  $[\text{M}(\text{N}\sim\text{N})_2(1,4\text{-xdpH}_2)(1,4\text{-xdpH}_4)]$  class.

In the absence of crystal field coordination preferences, the  $d^{10}$  Zn(II) structures exhibit coordination modes that approach both the square pyramidal and trigonal bipyramidal idealized

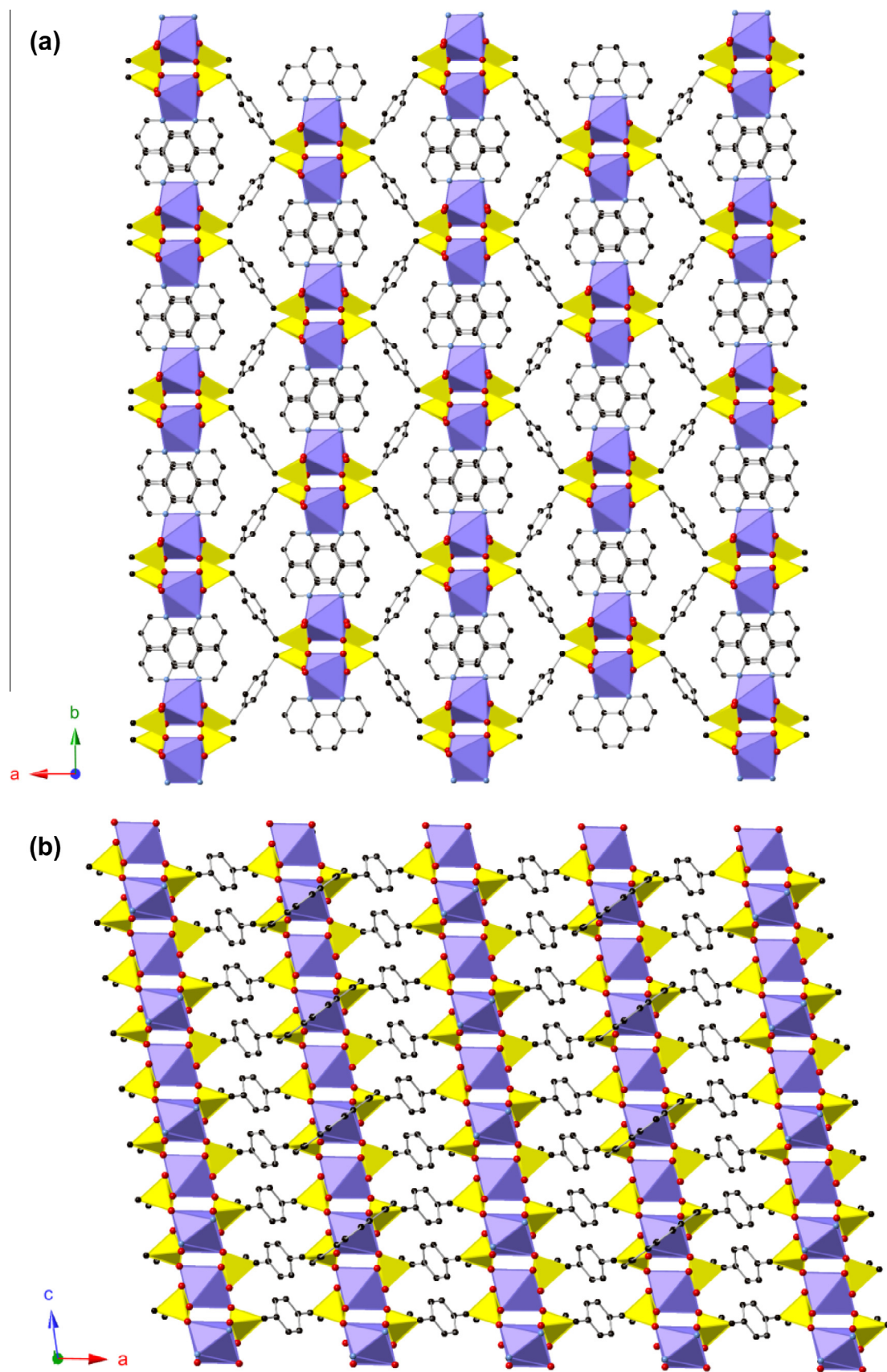


**Fig. 8.** (a) A view of the three-dimensional structure of [Cd(o-phen)(1,4-HO<sub>3</sub>PC<sub>8</sub>H<sub>8</sub>PO<sub>3</sub>H)] (12) in the *ab* plane; (b) a view of the linking of one-dimensional substructures through the xyllyl tethers of the diphosphonate ligands in the *ac* plane.

**Table 2**  
Summary of Selected Structural Characteristics of Xylyldiphosphonates with M(II)-organonitrogen chelate Moieties.

Molecular species <sup>a</sup>	M(II) coordination	Phosphonate bonding	Metal-phosphonate SBU
[Cu(H <sub>2</sub> O)(o-phen)(1,4-xdpH <sub>2</sub> )]	{CuN <sub>2</sub> O <sub>3</sub> } square pyramidal	one terminus bridges 2 Cu sites; one is pendant	di-μ(O,O') bridged {Cu <sub>2</sub> (RPO <sub>3</sub> ) <sub>2</sub> } ring
[Cu <sub>2</sub> (H <sub>2</sub> O) <sub>2</sub> (bpy)(1,4-xdpH <sub>3</sub> ) <sub>2</sub> (1,4-xdpH <sub>2</sub> )]	{CuN <sub>2</sub> O <sub>3</sub> } square pyramidal	one terminus bonds to a single Cu site; one is pendant	{Cu(RPO <sub>3</sub> ) <sub>2</sub> } unit
[Cu <sub>2</sub> (tpyprz)(1,2-xdpH <sub>2</sub> ) <sub>2</sub> ] [Cu <sub>4</sub> Cl <sub>4</sub> (tpyprz) <sub>2</sub> (1,4-xdpH <sub>3</sub> ) <sub>2</sub> Cl <sub>2</sub> ]	{CuN <sub>2</sub> O <sub>3</sub> } square pyramidal {CuN <sub>3</sub> OCl} square pyramidal	each terminus bonds to a single Cu site one terminus bridges 2 Cu sites; one is pendant	{Cu(RPO <sub>3</sub> ) <sub>2</sub> } unit μ(O,O') bridged {Cu <sub>2</sub> (RPO <sub>3</sub> ) <sub>2</sub> } unit
[Cu(2,2'-dpa)(1,3-xdpH <sub>2</sub> )]	{CuN <sub>2</sub> O <sub>2</sub> } square planar	one terminus bridges 2 Cu sites; one is pendant	di-μ(O,O') bridged {Cu <sub>2</sub> (RPO <sub>3</sub> ) <sub>2</sub> } ring
<i>One-dimensional structures</i>			
[Cu <sub>2</sub> (H <sub>2</sub> O) <sub>2</sub> (o-phen) <sub>2</sub> (1,4-xdpH <sub>2</sub> )]	{CuN <sub>2</sub> O <sub>3</sub> } square pyramid	each terminus bonds to two Cu sites	di-μ(O,O') bridged {Cu <sub>2</sub> (RPO <sub>3</sub> ) <sub>2</sub> } rings
[Zn(bpy)(H <sub>2</sub> O)(1,2-xdpH <sub>2</sub> )] [M(N~N)(1,3-xdpH <sub>2</sub> )] M = Cu, N~N = bpy, o-phen; M = Zn, N~N = bpy o-phen; M = Cd, N~N = o-phen	{ZnN <sub>2</sub> O <sub>3</sub> } trigonal bipyramid {MN <sub>2</sub> O <sub>3</sub> } square pyramid	each terminus bonds to one Zn site one terminus bridges two M sites; the second bonds to a single M site	{Zn(RPO <sub>3</sub> ) <sub>2</sub> } unit di-μ(O,O') bridged {M <sub>2</sub> (RPO <sub>3</sub> ) <sub>2</sub> } ring
[M(tpyprz)(1,2-xdpH <sub>2</sub> )] M = Co, Ni M = Zn	{MN <sub>3</sub> O <sub>3</sub> } octahedron {MN <sub>3</sub> O <sub>2</sub> } trigonal bipyramid	one terminus bridges two M sites; the second bonds to a single M site; each terminus bonds to one Zn site	di-μ(O,O') bridged {M <sub>2</sub> (RPO <sub>3</sub> ) <sub>2</sub> } ring {Zn(RPO <sub>3</sub> ) <sub>2</sub> } unit
[Ni <sub>2</sub> (tpyprz)(1,4-xdpH <sub>2</sub> )]	{MN <sub>3</sub> O <sub>3</sub> } octahedron	one terminus bridges two Ni sites; the second bonds to a single Ni site	di-μ(O,O') bridged {Ni <sub>2</sub> (RPO <sub>3</sub> ) <sub>2</sub> } ring
<i>Two-dimensional structures</i>			
[M(N~N)(1,2-xdpH <sub>2</sub> )] M = Mn, Co, Cu, Zn, Cd; N~N = o-phen. M = Mn; N~N = bpy	{MN <sub>2</sub> O <sub>3</sub> } square pyramid	one terminus bridges two M sites; the second bonds to a single M site	di-μ(O,O') bridged {M <sub>2</sub> (RPO <sub>3</sub> ) <sub>2</sub> } ring
[Cu(N~N)(1,4-xdpH <sub>2</sub> )] N~N = bpy N~N = o-phen	{CuN <sub>2</sub> O <sub>3</sub> } square pyramid {CuN <sub>2</sub> O <sub>3</sub> } square pyramid	each terminus of one diphosphonate bridges two Cu sites; each terminus of a second diphosphonate bonds to one Cu site One terminus bridges two Cu sites; the second bonds to a single Cu site	di-μ(O,O') bridged {Cu <sub>2</sub> (RPO <sub>3</sub> ) <sub>2</sub> } ring
[M(N~N)(1,3-xdpH <sub>2</sub> )] M = Mn, Co, Ni; N~N = bpy. M = Mn, Co Ni; N~N = o-phen	{MN <sub>2</sub> O <sub>4</sub> } octahedron	each terminus bridges two M sites	di-μ(O,O') bridged {M <sub>2</sub> (RPO <sub>3</sub> ) <sub>2</sub> } rings fused into a 1-D chain
[Cd(N~N)(xdpH <sub>2</sub> )] N~N = bpy; xdp = 1,3 xdp	{Cd(N <sub>2</sub> O <sub>4</sub> )} octahedron	each terminus bridges two Cd sites	di-μ(O,O') bridged {Cd <sub>2</sub> (RPO <sub>3</sub> ) <sub>2</sub> } rings fused into a 1D chain
[M(N~N) <sub>2</sub> (1,4-xdpH <sub>2</sub> )(1,4-xdpH <sub>4</sub> )] M = Mn, Zn, Cd; N~N = bpy. M = Co, Ni; N~N = o-phen	{M(N <sub>4</sub> O <sub>2</sub> )} octahedron	each terminus of one diphosphonate bonds to one M site; the second diphosphonate is involved in H-bonding only	{M(RPO <sub>3</sub> ) <sub>2</sub> } unit
<i>Three-dimensional structures</i>			
[Zn <sub>4</sub> (o-phen) <sub>4</sub> (1,4-xdpH <sub>2</sub> )(1,4-xdpH <sub>2</sub> )]	{Zn(N <sub>2</sub> O <sub>3</sub> )} distorted square pyramid	each terminus of both unique diphosphonates bridge two Zn sites	di-μ(O,O') bridged {Zn <sub>2</sub> (RPO <sub>3</sub> ) <sub>2</sub> } rings.
[M(o-phen)(1,4-xdpH <sub>2</sub> )] M = Co, Cd	{MN <sub>2</sub> O <sub>4</sub> } octahedron	each terminus bonds to two metal sites	di-μ(O,O') bridged {M <sub>2</sub> (RPO <sub>3</sub> ) <sub>2</sub> } rings fused into a 1D chain

<sup>a</sup> xdpH<sub>4</sub> = xylyldiphosphonate acid.

geometries. As expected, Cd(II) provided a number of materials where the coordination number expanded to six in distorted octahedral geometries of {CdN<sub>2</sub>O<sub>4</sub>} and {CdN<sub>5</sub>O<sub>2</sub>} types.

A number of persistent structural prototypes can be identified for specific xylyldiphosphonate geometries. The one-dimensional phases of the type [M(N~N)(1,3-xdpH<sub>2</sub>)] are observed for Cu(II), Zn(II) and Cd(II) with bpy and o-phen chelates. However, for Mn(II), Co(II) and Ni(II), two dimensional phases of the same overall composition [M(N~N)(1,3-xdpH<sub>2</sub>)] are observed. In both series of compounds, the core building unit is the {M<sub>2</sub>(di-μ-O,O-phosphonate)<sub>2</sub>} ring. However, in the one-dimensional series, these secondary building units are linked only through the xylyl tethers of the diphosphonate ligands, while in the two-dimensional series, these rings are directly fused into a chain substructure.

A rather obvious structural determinant is the relative locations of the methylenephosphonate groups on the ligand phenyl rings, whether 1,2-, 1,3- or 1,4-substituted. Thus, three dimensional structures are achieved only with the spatial expansion afforded by the 1,4-xylyldiphosphonate ligand in compounds **6** and **12**. The structures of these series also reflect the free rotation of the {PO<sub>3</sub>}<sup>2-</sup> or {PO<sub>3</sub>H}<sup>1-</sup> groups about the methylene carbon atoms. For example, in compounds **1**, **5–8**, **11** and **12**, the phosphate groups are disposed in the *syn* configuration with respect to the

phenyl rings while in the materials **2–4** and **9**, the substituents adopt the *anti* limiting geometry (Scheme 1). While these limiting geometries predominate in this study and are also apparent in the previously reported manganese, cobalt, nickel and copper series of xylyldiphosphonates [77,78], the rotational versatility of the ligand is manifested in the structure of compound **6** where one of the structurally independent 1,4-xylyldiphosphonate ligands adopts an intermediate geometry with one {PO<sub>3</sub>} group displaying the conventional distance between the phenyl plane and the phosphorus atom of ca. 1.75 Å and the second folding into the phenyl plane with a plane to phosphorus distance of ca. 0.45 Å.

The two-dimensional phases provide two additional structural prototypes, reflecting the identity of the xylyldiphosphonate ligand: [M(N~N)(1,2-xdpH<sub>2</sub>)] and the unusual [M(N~N)<sub>2</sub>(1,4-xdpH<sub>2</sub>)(2,4-xdpH<sub>2</sub>)]. The compounds incorporating the 1,2-xylyldiphosphonate ligand again exhibit the recurrent {M<sub>2</sub>(di-μ-O,O'-phosphonate)<sub>2</sub>} secondary building unit, and the network structure is observed for all metals of this study except Ni(II) for which no crystalline phases incorporating 1,2-xylyldiphosphonate were isolated in our studies. It is noteworthy that Co, Ni and Zn provide one-dimensional phases with 1,2-xylyldiphosphonate with the general formula [M(N~N)(1,2-xdpH<sub>2</sub>)]. However, zinc provides two distinct structural types, both based on isolated

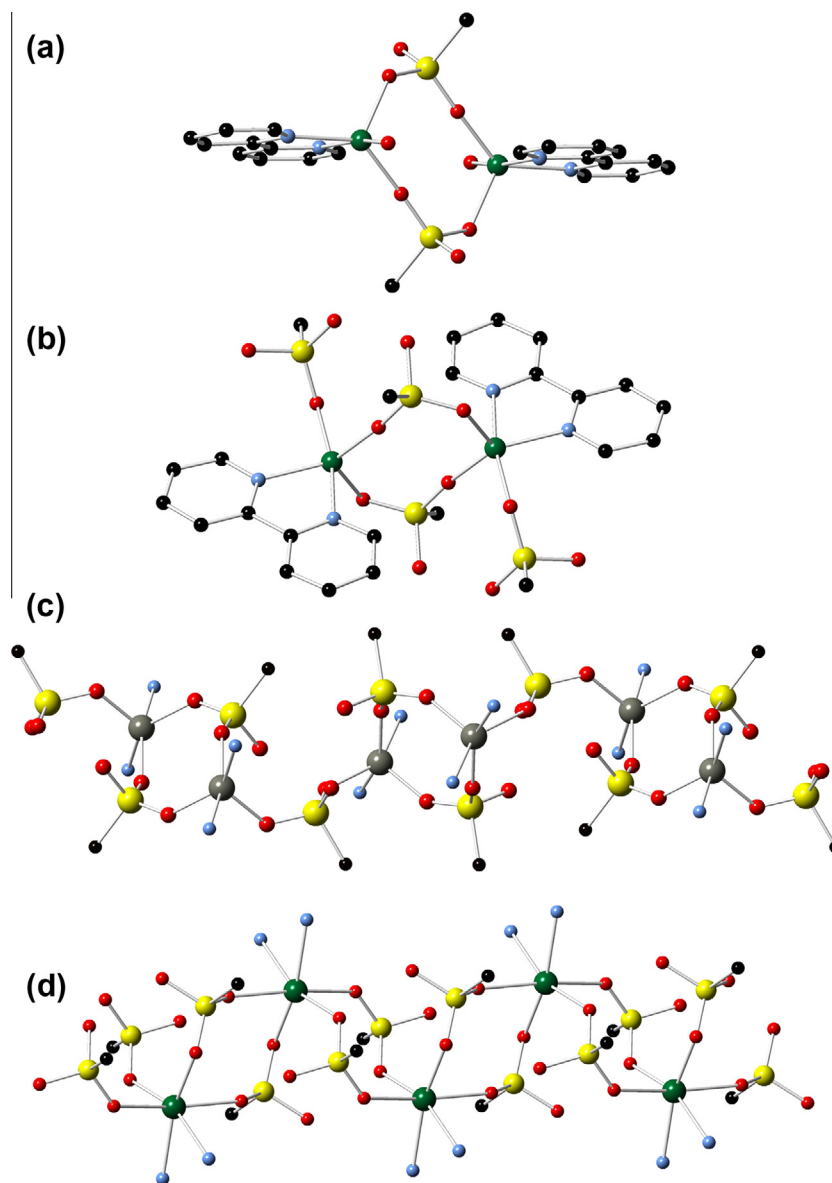


**Fig. 9.** (a) The di- $\mu$ -O,O'-phosphonate bridged metal binuclear core, showing the  $\{M_2P_2O_4\}$  ring; (b) the  $\{M_2(\text{ligand})_2(RPO_3)_4\}$  building block common to the one-dimensional compounds **2**·H<sub>2</sub>O, **5**·H<sub>2</sub>O, and **11** and to the two-dimensional materials **4** and **10**; (c) the one-dimensional substructure of **6**·3H<sub>2</sub>O; (d) the one-dimensional substructure of **8** and **12**.



**Scheme 1.** The *syn*, *anti* and intermediate configuration of the methylenephosphonate groups with respect to the phenyl rings of the xylyldiphosphonate ligands.

$\{Zn(RPO_3)_2\}$  units but with bpy and aqua coordination in one case and tpyrz ligation in the second.

The most unusual structural prototype is the virtual network adopted by the compounds  $[M(N\sim N)_2(1,4\text{-xdpH}_2)(1,4\text{-xdpH}_4)]$  where  $\{M(N\sim N)_2(1,4\text{-H}_2\text{O}_3\text{PC}_8\text{PO}_3\text{H}_2)\}_n^{2n+}$  chains are linked through hydrogen-bonding to  $\{\text{HO}_3\text{PC}_8\text{H}_8\text{PO}_3\text{H}\}^{2-}$  anions. The series spans all the metals of this study except Cu(II) whose coordination requirements are quite distinctive. In contrast to the Jahn–Teller distorted coordination environments of Cu(II), the other metals of this study readily adopt the more regular octahedral geometries that are required for these structures.

Three-dimensional structures are restricted to compounds incorporating the 1,4-xylyldiphosphonate ligand which appears

to provide sufficient extension to encapsulate the secondary chelating ligand within the framework structure. The most unusual example is  $[Zn_4(o\text{-phen})_4(1,4\text{-xdpH}_2)(1,4\text{-xdpH}_4)_2]$  which not only exhibits two distinct ligand protonation modes but also adopts a unique building unit consisting of  $\{M_2(\text{di-}\mu\text{-O,O'-phosphonate})_2\}$  clusters linked in turn through a single  $\mu\text{-O,O'-phosphonate}$  tetrahedra.

### 3.4. Thermal analyses

The TGA for compound **1** exhibits stability up to ca. 215 °C followed by a weight loss of ca. 37% at 425 °C, attributed to the loss of the 2,2'-bipyridine ligand and the coordinated water molecule (35%,

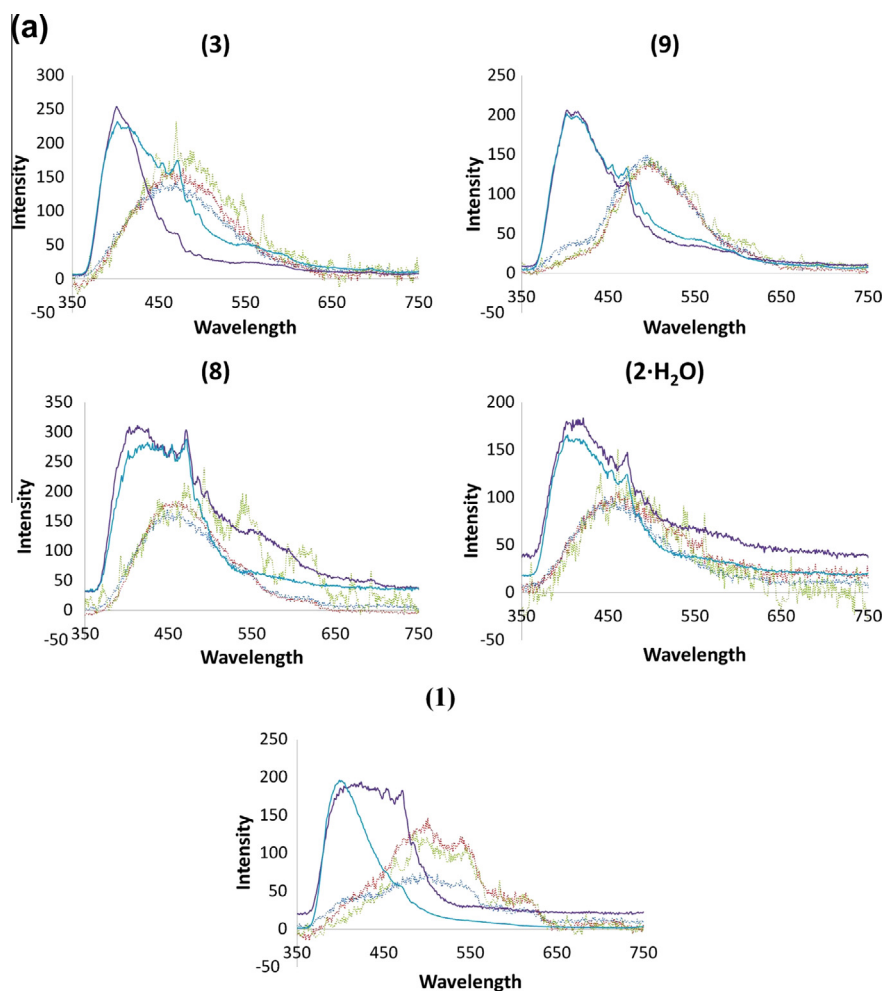


**Fig. 10.** The steady state total emission spectra at room temperature (purple) and 77 K (lightblue) compared to the gated detection spectra at 77 K with delay times of 1 ms (blue), 3 ms (red) or 10 ms (green) for the (a) 2,2'-bipyridine and (b) 1,10-phenanthroline compounds of this study. The compounds are identified by their assigned number on the plots. (For interpretation of the references to colour in this figure legend, the reader is referred to the web version of this article.)

theoretical). The compound is then stable up to 580 °C, followed by an additional weight loss of nearly 10% between 580 and 600 °C. This weight loss is most likely attributed to the partial decomposition of the diphosphonate ligand. The amorphous residue, most likely a zinc phosphate, is stable from about 610 °C to the temperature limit of the scan. Compound **6**·3H<sub>2</sub>O exhibits similar features in its respective TGA plot.

Compound **2**·H<sub>2</sub>O displays a weight decrease of about 4% attributed to the loss of the water of crystallization (calculated, 4%) between 25 °C to 205 °C. The compound is then stable until 300 °C, whereupon from 300 °C to 515 °C, the organonitrogen ligand is gradually lost, as shown by a weight loss of 31% (32%, theoretical). At 515 °C, a loss in weight of less than 5% is observed, which is most likely due to the initial decomposition of the diphosphonate ligand. The compound is then relatively stable from 675 to 800 °C.

Compound **3** is stable from 25 to 210 °C, whereupon there is a weight loss of 65% between 210 and 360 °C, which is attributed to the decomposition of the organonitrogen ligands and the hydrogen-bonded diphosphonate ligand (64%, calculated). The amorphous zinc phosphate residue is stable to the limit of the run, i.e., 800 °C.

Compound **4** exhibits no weight loss up to 310 °C. Between 310 and 620 °C a rapid weight loss is observed closely followed by a more gradual weight loss, corresponding to a total of ca. 85% of the original weight of sample. The weight loss is attributed to the decomposition of the organonitrogen ligand, followed by the initial degradation of the diphosphonate ligand. The amorphous

residue is stable from 620 to 800 °C. The TGA of compound **7** exhibits similar features to that of compound **4**.

Compound **5**·H<sub>2</sub>O experiences a gradual weight loss from 25 °C to 200 °C of ca. 5% attributed to the water of crystallization (calculated, 4%). Subsequently, there is a plateau of stability up to about 390 °C, which is then followed by a weight loss of 26% in the range 390–800 °C. This loss is most likely due to the degradation of the organonitrogen ligand, followed by the gradual decomposition of the diphosphonate ligand.

Compound **8** is stable up to about 250 °C, and then experiences a weight loss from 250 to 350 °C of about 35% attributed to the loss of the organonitrogen ligand (30%, calculated). An additional weight loss of about 20% occurs between 350 and 575 °C, which is due to the partial degradation of the diphosphonate ligand. The compound is then stable from about 575–800 °C. The TGA plots of compounds **9** and **10** exhibit similar features.

Compound **11** exhibits a gradual weight loss of about 20% between 375 and 800 °C which is attributed to the loss of the organonitrogen ligand. The TGA of compound **12** exhibits similar features.

### 3.5. Luminescence studies

The spectra presented in Fig. 10 are sorted by ligand and then by metal. The pairs of spectra shown side by side with Zn and Cd share the same phosphonate structure. In each case steady state

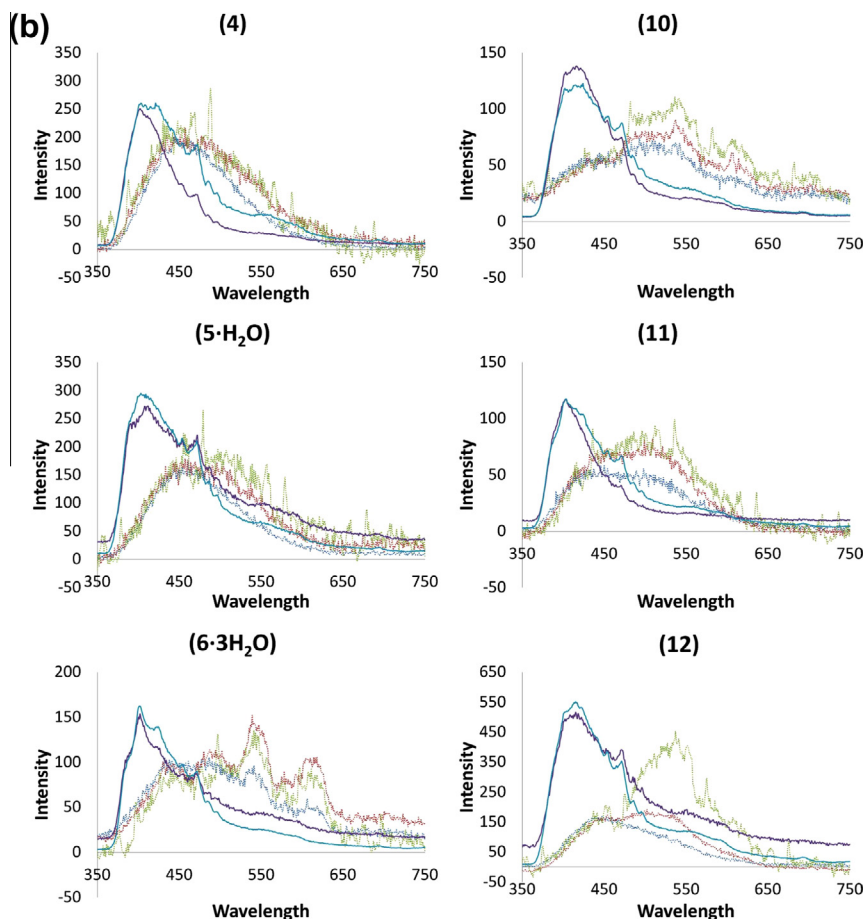


Fig. 10 (continued)

total emission spectra are shown at room temperature (purple) and at 77 K (light blue). These are compared on an arbitrary scale with spectra obtained by gated detection spectra obtained at 77 K following a delay of 1 ms (blue), 3 ms (red) or 10 ms (green). These “time-gated” spectra reveal long lived emission probably due to ligand phosphorescence or recombination luminescence. The steady state emission spectra will have added the signal from fluorescence of the ligand to this weak long-lived emission. In all cases the time-gated emission is at lower energy than the prompt steady state emission but only by at most  $5000\text{ cm}^{-1}$ . In four of the twelve cases the long lived emission, especially that obtained with 10 ms delay, exhibits structure that appears to be vibronic.

Comparison of the steady state spectra obtained at room temperature and at 77 K shows diverse behavior. In the 2,2'-bipyridine case three of the five spectra are virtually superimposable at the two temperatures, one shows a longer red emission at room temperature and the other at low temperature. All of these 2,2'-bipyridine steady state spectra exhibit what looks like structure that may be due to the long lived emission. In the case of the *o*-phenanthroline compounds, the steady state spectra are similar, indicative of similar vibronic structure. The case of the tetra-2-pyridinylpyrazine structure,  $[\text{Zn}(\text{tpyprz})(1,2\text{-HO}_3\text{PC}_8\text{H}_8\text{PO}_3\text{H})]$  (7), is perhaps of most interest in that the lower energy emission increases at low temperature and the vibrational structure observed at room temperature is repeated at low temperature.

In several cases, most clearly for the 2,2'-bipyridine case  $[\text{Cd}(\text{bpy})(1,3\text{-HO}_3\text{PC}_8\text{H}_8\text{PO}_3\text{H})]$  (8) and for the tetra-2-pyridinylpyrazine case  $[\text{Zn}(\text{tpyprz})(1,2\text{-HO}_3\text{PC}_8\text{H}_8\text{PO}_3\text{H})]$  (7), the structured part of the time-gated spectrum, especially that obtained with

the longest delay of 10 ms, appears to be red shifted relative to, and superimposed on, a more continuous shorter lived emission. When the longer delay changes the spectrum the new features are structured and are predominantly at longer wave length.

A previous study on the behavior of 2,2'-bipyridine in solution reported the fluorescence of both 2,2'-bipyridine and the complexes with cadmium and zinc [84]. Upon complexation of 2,2'-bipyridine with the metal(II) species, the lowest excited singlet state was assigned to the ligand. Consequently, there is no change in spectral behavior when compared with that of the ligand in the 320–500 nm spectral region. This lowest excited singlet state is due to a  $\pi\pi^*$  transition with a  $\lambda_{\text{cm}} = 328\text{ nm}$ . The complexes of 2,2'-bipyridine with zinc(II) and cadmium(II) yield excitation maxima in the 365–370 nm range with the fluorescence maxima red shifted to the 430–455 nm range.

The present set of spectra appear to be explained by the superposition of ligand fluorescence with long lived structured ligand phosphorescence. There are several considerations that should be kept in mind in the description of emission spectra of crystalline solids. The first is that energy transfer is likely to be rapid for the singlet excitations and slow for the triplet excitations at low temperature. This raises the point that it is always possible that the emission is due to defect states of lower energy. The similarity of the spectra for all compounds with a given ligand argues that this last feature is not likely for the fluorescence component in these cases. The present set of spectra appear to be explained as superposition of fluorescence and one or two components of a long-lived emission. One of these is nearly continuous in its spectral shape and does not depend appreciably on the initial time of the

time-gate. This is the dominant component for most of the materials studied. For  $[\text{Cd}(\text{bpy})_2(1,4\text{-H}_2\text{O}_3\text{PC}_8\text{H}_8\text{PO}_3\text{H}_2)(1,4\text{-HO}_3\text{PC}_8\text{H}_8\text{PO}_3\text{H})]$  (**9**) this is the only component. This emission is close in spectral position to the fluorescence. This is attributed to delayed fluorescence due either to triplet recombination or to recombination luminescence. For  $[\text{Zn}(\text{H}_2\text{O})(\text{bpy})(1,2\text{-HO}_3\text{PC}_8\text{H}_8\text{PO}_3\text{H})]$  (**1**),  $[\text{Cd}(\text{bpy})(1,3\text{-HO}_3\text{PC}_8\text{H}_8\text{PO}_3\text{H})]$  (**8**),  $[\text{Cd}(\text{o-phen})(1,2\text{-HO}_3\text{PC}_8\text{H}_8\text{PO}_3\text{H})]$  (**10**),  $[\text{Zn}_4(\text{o-phen})_4(1,4\text{-HO}_3\text{PC}_8\text{H}_8\text{PO}_3)_2(1,4\text{-HO}_3\text{PC}_8\text{H}_8\text{PO}_3\text{H})]$  (**6**· $3\text{H}_2\text{O}$ ),  $[\text{Cd}(\text{o-phen})(1,4\text{-HO}_3\text{PC}_8\text{H}_8\text{PO}_3\text{H})]$  (**12**) and  $[\text{Zn}(\text{tpyprz})(1,2\text{-HO}_3\text{PC}_8\text{H}_8\text{PO}_3\text{H})]$  (**7**) there is an additional structured emission that is relatively enhanced by longer delay times. The compound  $[\text{Cd}(\text{bpy})(1,3\text{-HO}_3\text{PC}_8\text{H}_8\text{PO}_3\text{H})]$  (**8**) is a case where the emission clearly has two components. Furthermore, compound  $[\text{Zn}(\text{tpyprz})(1,2\text{-HO}_3\text{PC}_8\text{H}_8\text{PO}_3\text{H})]$  (**7**) is a case where this structured emission dominates and appears to have a lifetime in the 3 ms range.

#### 4. Conclusions

Hydrothermal methods have been exploited to prepare twelve new members of the general class of materials  $\text{M}(\text{II})(\text{N}\sim\text{N})/\text{xylyldiphosphonate}$  where  $\text{M}(\text{II})$  is  $\text{Zn}(\text{II})$  and  $\text{Cd}(\text{II})$  and  $\text{N}\sim\text{N}$  represents a chelating organonitrogen ancillary ligand. The incorporation of the ancillary ligands prevents the formation of the common pillared layer structural prototype for metal-diphosphonate phases by reducing the number of available coordination sites about the metal centers.

As noted previously for the  $\text{Mn}(\text{II})$ ,  $\text{Co}(\text{II})$ ,  $\text{Ni}(\text{II})$  and  $\text{Cu}(\text{II})$  materials constructed with xylyldiphosphonate and ancillary organonitrogen chelating ligands, one- and two-dimensional structures predominate. However, when 1,4-xylyldiphosphonate is used, the ligand spatial extension is sufficient to allow encapsulation of the ancillary ligands within a three-dimensional framework, affording several examples of novel extended structural motifs. These framework structures are quite distinct from the pillared layered prototypes.

It is also noteworthy that a number of recurrent structural motifs can be identified. These include the one-dimensional  $[\text{M}(\text{N}\sim\text{N})(1,3\text{-HO}_3\text{PC}_8\text{H}_8\text{PO}_3\text{H})]$ , the virtual two-dimensional phases  $[\text{M}(\text{N}\sim\text{N})_2(1,4\text{-H}_2\text{O}_3\text{PC}_8\text{H}_8\text{PO}_3\text{H}_2)(1,4\text{-HO}_3\text{PC}_8\text{H}_8\text{PO}_3\text{H})]$ , and the two-dimensional families of materials  $[\text{M}(\text{N}\sim\text{N})(1,2\text{-HO}_3\text{PC}_8\text{H}_8\text{PO}_3\text{H})]$  and  $[\text{M}(\text{N}\sim\text{N})(1,3\text{-HO}_3\text{PC}_8\text{H}_8\text{PO}_3\text{H})]$ . A short series of three-dimensional phases  $[\text{M}(\text{o-phen})(1,4\text{-HO}_3\text{PC}_8\text{H}_8\text{PO}_3\text{H})]$  has also been identified. For these recurrent structural types, it is evident that the identity of the xylyldiphosphonate ligand is a critical structural determinant.

However, the structural variety encountered in the general class of  $\text{M}(\text{II})$ -organonitrogen chelate/xylyldiphosphonate compounds also reflects a number of additional structural determinants, including accessibility of different coordination polyhedra, variable aqua coordination, variable protonation and coordination of phosphonate oxygen atoms, the flexibility of the  $\text{M}-\text{O}-\text{P}$  valence angles, and the interplay of relative ligand sizes, geometries and denticities. Furthermore, reaction conditions such as stoichiometry, temperature and pH are important factors in determining the product composition and structure.

#### Acknowledgement

This work was funded by a grant from the National Science Foundation (CHE-0907787).

#### Appendix A. Supplementary material

CCDC 942844–942855 contains the supplementary crystallographic data for **1–12**. These data can be obtained free of charge from The Cambridge Crystallographic Data Centre via

[www.ccdc.cam.ac.uk/data\\_request/cif](http://www.ccdc.cam.ac.uk/data_request/cif). Supplementary data associated with this article can be found, in the online version, at <http://dx.doi.org/10.1016/j.ica.2013.12.003>.

#### References

- [1] C. Janiak, *Dalton Trans.* (2003) 2781, and references therein.
- [2] S.M. Cohen, *Chem. Rev.* 112 (2012) 970.
- [3] M. O'Keeffe, O.M. Yaghi, *Chem. Rev.* 112 (2012) 675.
- [4] M.P. Suk, H.J. Park, T.K. Prasad, D.M. Lim, *Chem. Rev.* 112 (2012) 782.
- [5] K. Sumida, D.L. Rogow, J.A. Mason, T.M. McDonald, E.D. Block, Z.R. Herm, T.H. Bae, J.R. Long, *Chem. Rev.* 112 (2012) 724.
- [6] L. Ma, C. Alney, W.B. Lin, *Chem. Soc. Rev.* 38 (2009) 1248.
- [7] C. Wang, T. Zhang, W.B. Lin, *Chem. Rev.* 112 (2012) 1084.
- [8] M. Kurmoo, *Chem. Soc. Rev.* 38 (2009) 1353.
- [9] D.B. Mitzi, *J. Chem. Soc., Dalton Trans.* (2001) 1.
- [10] See for example M. Hmadeh, Z. Lu, Z. Liu, F. Gandara, H. Furukawa, S. Wan, V. Agustyn, Veronica, R. Chang, L. Liao, F. Zhou, O.M. Yaghi, *Chem. Mater.* 24 (2012) 3511 (and also refs. 11–15).
- [11] P. Horcajada, R. Gref, T. Baati, P.K. Allan, G. Maurin, P. Couvreur, G. Férey, *Chem. Rev.* 112 (2012) 1232.
- [12] G. Férey, *Chem. Soc. Rev.* 37 (2008) 191.
- [13] E. Procopio, T. Fukushima, E. Barea, J.A.R. Navarro, S. Horike, S. Kitagawa, *Chem. Eur. J.* 18 (2012) 13117.
- [14] X. Kong, E. Scott, W. Ding, J.A. Mason, J.R. Long, J.A. Reimer, *J. Am. Chem. Soc.* 134 (2012) 14341.
- [15] W. Ouellette, M.H. Yu, C.J. O'Connor, D. Hagrman, J. Zubieta, *Angew. Chem., Int. Ed.* 45 (2006) 3497.
- [16] A. Clearfield, *Prog. Inorg. Chem.* 47 (1998) 371.
- [17] A. Clearfield, *Dalton Trans.* (2008) 6089.
- [18] A. Clearfield, K.D. Demadis (Eds.), *Metal Phosphonate Chemistry from Synthesis to Applications*, Royal Society of Chemistry, Cambridge, UK, 2012.
- [19] A. Vioux, J. LeBideau, P.H. Mutin, D. Leclercq, *Top. Curr. Chem.* 232 (2004) 145.
- [20] A. Clearfield, *Curr. Opin. Solid State Mater. Sci.* 6 (2002) 495.
- [21] A. Clearfield, in: J.L. Atwood, J.E.D. Davies, F. Vogt (eds.), *Comprehensive Supramolecular Chemistry*, vol. 9, Pergamon Press, New York, 1996, p. 107.
- [22] A. Clearfield, *Chem. Mater.* 10 (1998) 2801.
- [23] S. Konar, A.V. Prosvirin, K.R. Dunbar, A. Clearfield, *Inorg. Chem.* 46 (2007) 5229.
- [24] J.W. Johnson, A.J. Jacobson, W.M. Butler, S.E. Rosenthal, J.F. Brody, J.T. Lewandowski, *J. Am. Chem. Soc.* 111 (1989) 381.
- [25] S. Jones, J. Zubieta in: A. Clearfield, K.D. Demadis (eds.), *Metal Phosphonate Chemistry from Synthesis to Applications*, vol. 7, Royal Society of Chemistry, Cambridge, UK, 2013, p. 192.
- [26] K. Maeda, *Microporous Mesoporous Mater.* 73 (2004) 47.
- [27] G. Alberti, M. Casiola, U. Costantino, R. Vivani, *Adv. Mater.* 8 (1996) 291.
- [28] L.A. Vermeulen, *Prog. Inorg. Chem.* 44 (1997) 143.
- [29] G. Albert, in: J.L. Atwood, J.E.D. Davies, F. Vogt (eds.), *Comprehensive Supramolecular Chemistry*, Pergamon Press, New York 1996.
- [30] R.C. Finn, J. Zubieta, R.C. Haushalter, *Prog. Inorg. Chem.* 51 (2003) 451.
- [31] A. Clearfield, *Inorganic Ion Exchange Materials*, CRC Press, Boca Raton, FL, 1982.
- [32] A. Hu, H. Ngo, W. Lin, *J. Am. Chem. Soc.* 125 (2003) 11490.
- [33] K. Meada, *Microporous Mesoporous Mater.* 73 (2004) 47.
- [34] Z.-Y. Du, H.-B. Xu, J.-G. Mao, *Inorg. Chem.* 45 (2006) 6424.
- [35] P. Ayzappan, O.R. Evans, Y. Cui, K.A. Wheeler, W. Lin, *Inorg. Chem.* 41 (2002) 4978.
- [36] A. Anillo, A. Altomare, A.G.G. Moliterni, E.M. Bauer, C. Bellitto, M. Colapietro, G. Portalone, G. Righini, *J. Solid State Chem.* 178 (2001) 306.
- [37] G. Nenert, U. Adem, E.M. Bauer, C. Bellitto, G. Righini, T.T.M. Palstra, *Phys. Chem. Rev. B Cond. Mat. Mater. Phys.* 78 (2008) 054443/1.
- [38] G. Nenert, H.-J. Koo, C.V. Colin, E.M. Bauer, C. Bellitto, C. Ritter, G. Righini, M.-H. Whangbo, *Inorg. Chem.* 52 (2013) 753.
- [39] P. DeBurgomaster, W. Ouellette, H. Liu, C.J. O'Connor, J. Zubieta, *Cryst. Eng. Commun.* 12 (2010) 446.
- [40] R. Finn, J. Zubieta, *Chem. Commun.* (2000) 1821.
- [41] P.J. Hagrman, R.C. Finn, J. Zubieta, *Solid State Sci.* 3 (2001) 745.
- [42] R.C. Finn, J. Zubieta, *J. Phys. Chem. Solids* 62 (2001) 1513.
- [43] R.C. Finn, J. Zubieta, *J. Chem. Soc., Dalton Trans.* (2002) 856.
- [44] R.C. Finn, R. Lam, J.E. Greedan, J. Zubieta, *Inorg. Chem.* 40 (2001) 3745.
- [45] W. Ouellette, B.-K. Koo, E. Burkholder, V. Golub, C.J. O'Connor, J. Zubieta, *Dalton Trans.* (2004) 1527.
- [46] G. Yucesan, V. Golub, C.J. O'Connor, J. Zubieta, *Dalton Trans.* (2005) 2241.
- [47] G. Yucesan, N.G. Armatas, J. Zubieta, *Inorg. Chim. Acta* 359 (2006) 4557.
- [48] G. Yucesan, M.H. Yu, C.J. O'Connor, J. Zubieta, *Cryst. Eng. Commun.* 7 (2005) 711.
- [49] G. Yucesan, M.H. Yu, C.J. O'Connor, J. Zubieta, *Cryst. Eng. Commun.* 7 (2005) 480.
- [50] G. Yucesan, V. Golub, C.J. O'Connor, J. Zubieta, *Dalton Trans.* (2005) 7241.
- [51] G. Yucesan, W. Ouellette, V. Golub, C.J. O'Connor, J. Zubieta, *Solid State Sci.* 7 (2005) 445.
- [52] G. Yucesan, V. Golub, C.J. O'Connor, J. Zubieta, *Solid State Sci.* 7 (2005) 133.
- [53] G. Yucesan, J.E. Valeich, H. Liu, W. Ouellette, C.J. O'Connor, J. Zubieta, *Inorg. Chim. Acta* 362 (2010) 1831.

- [54] W. Ouellette, G. Wang, H. Liu, G.T. Lee, C.J. O'Connor, J. Zubieta, *Inorg. Chem.* **48** (2009) 953.
- [55] W. Ouellette, V. Golub, C.J. O'Connor, J. Zubieta, *Dalton Trans.* (2005) 291.
- [56] W. Ouellette, V. Golub, C.J. O'Connor, J. Zubieta, *J. Solid State Chem.* **180** (2007) 2500.
- [57] W. Ouellette, M.H. Yu, C.J. O'Connor, J. Zubieta, *Inorg. Chem.* **45** (2006) 7628.
- [58] N.G. Armatas, W. Ouellette, K. Whitenack, J. Pelcher, H. Liu, E. Romaine, C.J. O'Connor, J. Zubieta, *Inorg. Chem.* **48** (2009) 8897.
- [59] P. DeBurgomaster, A. Aldous, H. Liu, C.J. O'Connor, J. Zubieta, *Cryst. Growth Des.* (2010) 2209.
- [60] M. Bartholomae, H. Chueng, S. Pellizzeri, K. Ellis-Guardiola, S. Jones, J. Zubieta, *Inorg. Chim. Acta* (2012) 90.
- [61] D.M. Poorjary, B. Zhang, A. Clearfield, *Chem. Mater.* **11** (1999) 421.
- [62] D.I. Arnold, X. Ouyang, A. Clearfield, *Chem. Mater.* **14** (2002) 2020.
- [63] D.M. Poorjary, B. Zhang, A. Clearfield, *J. Am. Chem. Soc.* **119** (1997) 12550.
- [64] D.M. Poorjary, B. Zhang, P. Bellinghausen, A. Clearfield, *Inorg. Chem.* **35** (1996) 4942.
- [65] D. Knog, J. Zn, J. McBee, A. Clearfield, *Inorg. Chem.* **45** (2006) 977.
- [66] D. Kong, Y. Li, J.H. Ross, R.A. Clearfield, *Chem. Commun.* (2003) 1720.
- [67] M.M. Gomez-Alcantara, A. Cabeza, M. Martinez-Lara, M.A.G. Aranda, R. Suau, N. Bhuvanesh, A. Clearfield, *Inorg. Chem.* **43** (2004) 5283.
- [68] APEX2, Data Collection Software, version 2011.8-0, Bruker-AXS Inc., Madison, WI, 2011.
- [69] SMART, Data Collection Software, version 5.630, Bruker-AXS Inc., Madison, WI, 1997–2002.
- [70] SAINT plus, Data Reduction Software, version 6.45A, Bruker-AXS Inc., Madison, WI, 1997–2002.
- [71] G.M. Sheldrick, *SADABS*, University of Göttingen, 1996.
- [72] SHELXTL PC, version 6.12, Bruker-AXS Inc., Madison, WI, 2002.
- [73] CrystalMaker<sup>®</sup>: a crystal and molecular structures program. CrystalMaker Software Ltd., Oxford, England, [www.crystalmaker.com](http://www.crystalmaker.com).
- [74] R.M. Barrer, *Hydrothermal Chemistry of Zeolites*, Academic Press, London, 1982.
- [75] A.N. Lobachev, G.D. Archand, *Crystallization Processes Under Hydrothermal Conditions*, Consultants Bureau, New York, 1973.
- [76] M.S. Whittingham, *Curr. Opin. Solid State Mater. Sci.* **1** (1996) 227.
- [77] R.A. Laudise, *Chem. Eng. News* **65** (1987) 30.
- [78] J. Gopalakrishnan, *Chem. Mater.* **7** (1995) 1265.
- [79] J. Zubieta, Solid-state methods, hydrothermal, in: J.A. McCleverty, T.J. Meyer (eds.), *Comprehensive Coordination Chemistry II*, vol. 1, Elsevier Science, New York, 2004, p. 697.
- [80] T.M. Smith, J. Vargas, D. Symester, M. Tichenor, C.J. O'Connor, J. Zubieta, *Inorg. Chim. Acta*, <http://dx.doi.org/10.1016/j.ica.2013.01.001>.
- [81] T.M. Smith, D. Symester, K. Perrin, J. Vargas, M. Tichenor, C.J. O'Connor, J. Zubieta, *Inorg. Chim. Acta* **402** (2013) 46.
- [82] D. Riou, F. Belier, C. Serre, M. Nogues, D. Vichard, G. Ferey, *Int. J. Inorg. Mater.* **2** (2000) 29.
- [83] V. Chandrasekhar, T. Senapati, A. Dey, S. Hossain, *Dalton Trans.* **40** (2011) 5394.
- [84] S.J. Dhanya, *Photochem. Photobiol. A: Chem.* **1** (63) (1992) 179.